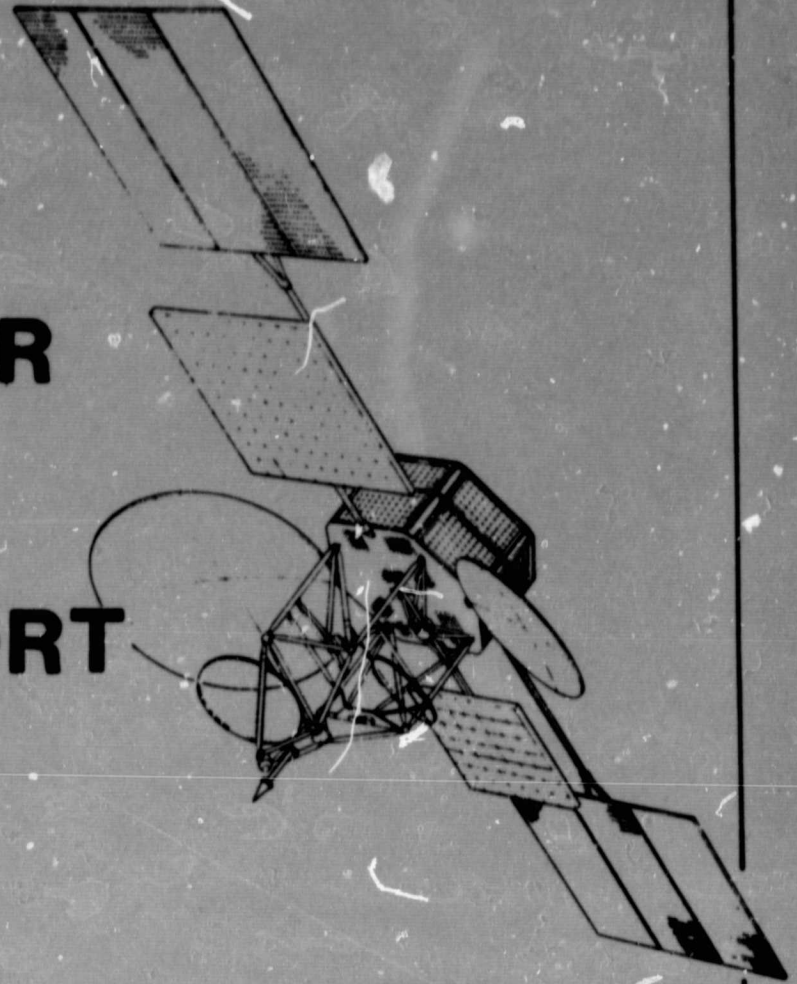


N O T I C E

THIS DOCUMENT HAS BEEN REPRODUCED FROM
MICROFICHE. ALTHOUGH IT IS RECOGNIZED THAT
CERTAIN PORTIONS ARE ILLEGIBLE, IT IS BEING RELEASED
IN THE INTEREST OF MAKING AVAILABLE AS MUCH
INFORMATION AS POSSIBLE

K-BAND HIGH POWER LATCHING SWITCH FINAL REPORT



DECEMBER 1980

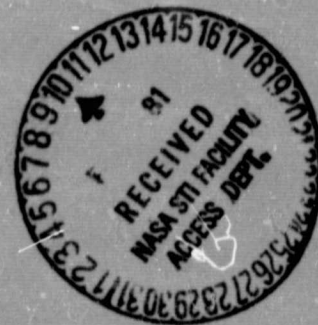
Prepared for:

NATIONAL AERONAUTICS AND
SPACE ADMINISTRATION

Lewis Research Center
2100 Brookpark Road
Cleveland, Ohio 44135

Sales Number 34037

Contact Number NAS 3-21761



(NASA-CR-165159) K-BAND HIGH POWER LATCHING
SWITCH Final Report (TRW Systems Group)
49 p HC A03/MF A01 CSCL 09A

N81-16389

Unclas

G3/33 41204

TRW
DEFENSE AND SPACE SYSTEMS GROUP

ONE SPACE PARK REDONDO BEACH CALIFORNIA 90278

PREFACE

The work described in this report was performed in the Microwave Technology Department of the Electronic Systems Division of TRW Defense and Space Systems Group. The work was performed under the direction of Dr. T. T. Fong, who gratefully acknowledges the principal contributions of Mr. Godfrey Anzic of the NASA-Lewis Research Center and Dr. J. E. Raue, Messrs. W. M. Brunner, M. J. Mlinar, and W. S. Piotrowski of TRW.

CONTENTS

	Page
1. INTRODUCTION AND SUMMARY	1
2. DESIGN CONSIDERATIONS	
2.1 Introduction	4
2.2 RF Design	4
2.3 Driver Design	7
2.4 Computer Aided Design	9
3. SWITCH DEVELOPMENT	
3.1 Introduction	11
3.2 Instrumentation	11
3.3 Fixed Junction Circulator	15
3.4 Latching Switch Development	17
3.5 Switch Actuating Development	22
3.6 Shock and Vibration	26
3.7 Thermal Test	38
4. CONCLUSION	43

TABLE OF FIGURES

<u>Figure Number</u>		<u>Page</u>
1	K-Band Latching Switch	3
2a	Complete Set of Ferrite Junction Piece Parts	5
2b	Cross-Section of Circulator Showing Junction Assembly	5
3	Cross-Section of Switching Junction Showing RF and Driver Ferrite Locations	6
4	Driver Assembly for Switch	7
5	Magnetic Loop of Switching Junction	8
6	Hysteresis Loop of Switch with Two Sets of Drivers	9
7	Sample Output of Circulator Design Program	10
8	Schematic of K-Band Development Circuit	12
9a	VSWR of Detector	13
9b	Detector Only	13
9c	Detector with attenuator	13
10	Degradation of Circulator Isolation with Load VSWR	14
11	VSWR of TRW Load	14
12	Final Performance of Non-Switching K-Band Circulator	16
13	Housing Design for K-Band Switch	18
14	Final Performance of K-Band Latching Switch (-1)	19
15	Final Performance of K-Band Latching Switch (-2)	21
16	Schematic of Latching Switch Actuating Circuitry	23
17	Board Layout of Switch Actuating Circuitry	24
18	Internal View of Actuating Board	25
19a	K-Band Switch Vibration Test Data: X-Axis	28
19b	K-Band Switch Vibration Test Data: Y-Axis	29
19c	K-Band Switch Vibration Test Data: Z-Axis	30
20a	K-Band Switch Shock Test Data: + X Axis	31
20b	K-Band Switch Shock Test Data: - X Axis	32
20c	K-Band Switch Shock Test Data: + Y Axis	33
20d	K-Band Switch Shock Test Data: - Y Axis	34
20e	K-Band Switch Shock Test Data: +Z Axis	35
20f	K-Band Switch Shock Test Data: -Z Axis	36
21	Switch Performance after Shock and Vibration Tests(-2)	37
22a	Performance of K-Band Switch Under Thermal (-1) with Port 1 as Input.	39
22b	Performance of K-Band Switch Under Thermal (-1) with Port 2 as Input.	40
22c	Performance of K-Band Switch Under Thermal (-1) with Port 3 as Input.	41
23	Switch Performance after Thermal Test	42

Table Number

Page

1	K-Band Switch Performance	2
2	Normalized Comparison of Non-Switching Junction Dimensions	15
3	Interface Data for K-Band Switch	20
4	Shock and Vibration Test Program	26

1. INTRODUCTION AND SUMMARY

This final report describes the study, design, development, and test results of a high power, low loss, K-band switch suitable for space applications.

This development effort is of significance to NASA as it provides for high power latching switches which will be required in 20/30 GHz communication satellite systems. Specifically, a waveguide latching switch with a bandwidth of 1300 MHz at an insertion loss of 0.25 dB was demonstrated. This type of component has been developed at X-band, tested, and qualified for use in a space vehicle.

The period of performance was originally 27 February 79 to 10 June 80. Delivery of the switch was extended to 19 August 80 due to delays in material delivery and development complications. The first switch was delivered in mid-August; the second unit was developed further, resulting in improved performance. Table 1 specifies the design goals for these devices and lists the performance achieved. The proposed switch design was a natural extension of a highly successful high power X-band latching switch that was qualified for space applications early in 1978. This component demonstrated extraordinary performance over band and was recently adapted for use in the LANDSAT program. The design for a switch at 19 GHz was extended from this X-band model.

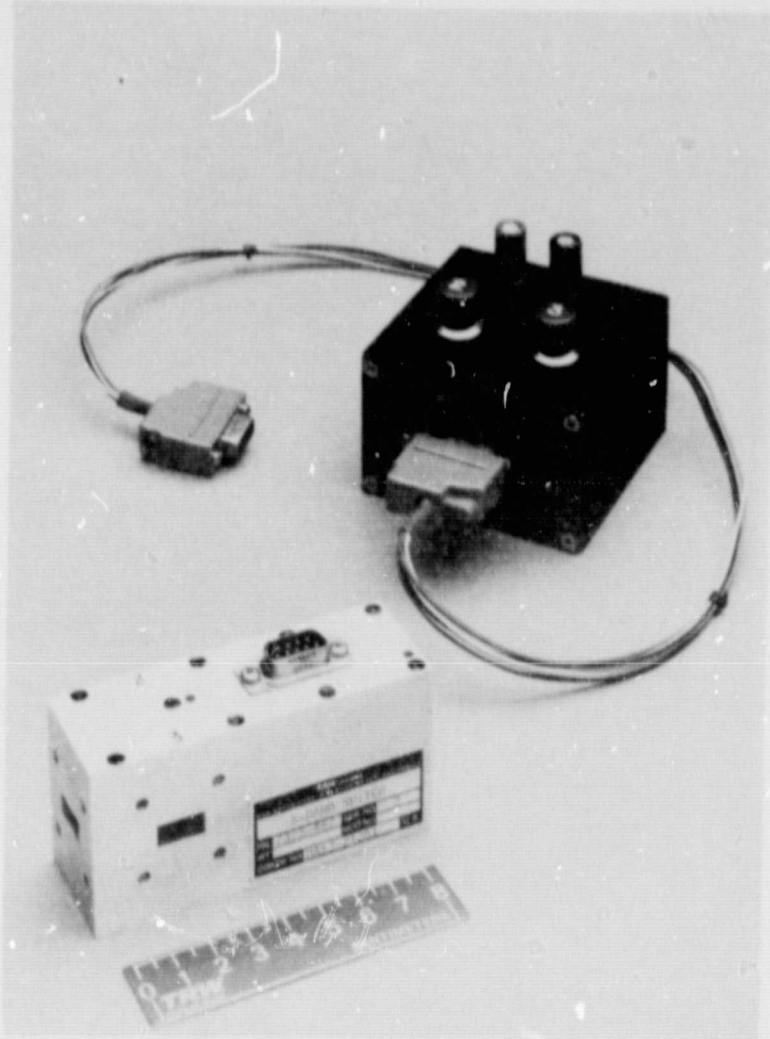
A photograph of the K-band switch is shown in Figure 1. For an application involving redundant TWTA's, the input port would be to the right and on its opposite side (not visible). The output port would be to the left. Note the compact design with a single 9 pin plug for power and switching; the actuating circuitry is located within the housing.

This report is organized as follows: Section 2 details the design considerations of the switching junction and Section 3 describes the development of the fixed and switching junction, as well as actuating circuitry and testing. Overall conclusions and recommendations are contained in Section 4.

Table 1. K-Band Switch Performance

PARAMETER	PERFORMANCE SPECIFICATIONS		ACTUAL	
	-1	-2	-1	-2
CENTER OPERATING FREQUENCY	18.95 GHz	19.1 GHz	18.95 GHz	19.1 GHz
BANDWIDTH	1.4 GHz	1.4 GHz	1.3 GHz	1.4 GHz
INSERTION LOSS	0.25 dB	0.25 dB	0.25 dB	0.25 dB
INSERTION LOSS FLATNESS	± 0.05 dB	± 0.05 dB	± 0.05 dB	± 0.05 dB
ISOLATION	25 dB	25 dB	21 dB	25 dB
INPUT VSWR	1.2:1	1.2:1	1.2:1	1.2:1
INPUT VSWR WITH 1.15:1 LOAD	1.3:1	1.3:1	1.15:1 TYPICAL OVER BAND 1.3:1 ON EDGE	1.15 TYP. OVER BAND 1.2 ON EDGE
CW OPERATING POWER	50-100 W	50-100 W	NOT MEASURED*	NOT MEASURED*
PHASE LINEARITY	$\pm 5^\circ$ OVER ANY 300 MHz PASSBAND SEGMENT	$\pm 5^\circ$ OVER ANY 300 MHz PASSBAND SEGMENT	DSCS-II SWITCHES SHOWED NEGLIGIBLE DEVIATION FROM PHASE LINEARITY	
SWITCHING TIME	80 μ sec	50 μ sec	50 μ sec	50 μ sec
MAX OPERATING TEMPERATURE	+56°C	+56°C	+56°C	+56°C
MINIMUM NON-OPERATING TEMPERATURE	-40°C	NOT TESTED	NOT TESTED	-44°C (OPERATING)

*TESTS NOT REQUIRED AND NOT PERFORMED DUE TO UNAVAILABILITY OF SUITABLE RF POWER SOURCES



168625-80

Figure 1. K-Band Latching Switch

2. DESIGN CONSIDERATIONS

2.1 Introduction

The design approach to the waveguide RF latching switch is described in this section. In the novel TRW design, the RF and driver ferrites are separate structures and, thus, can be optimized individually. The analysis for each structure is separately detailed in this section.

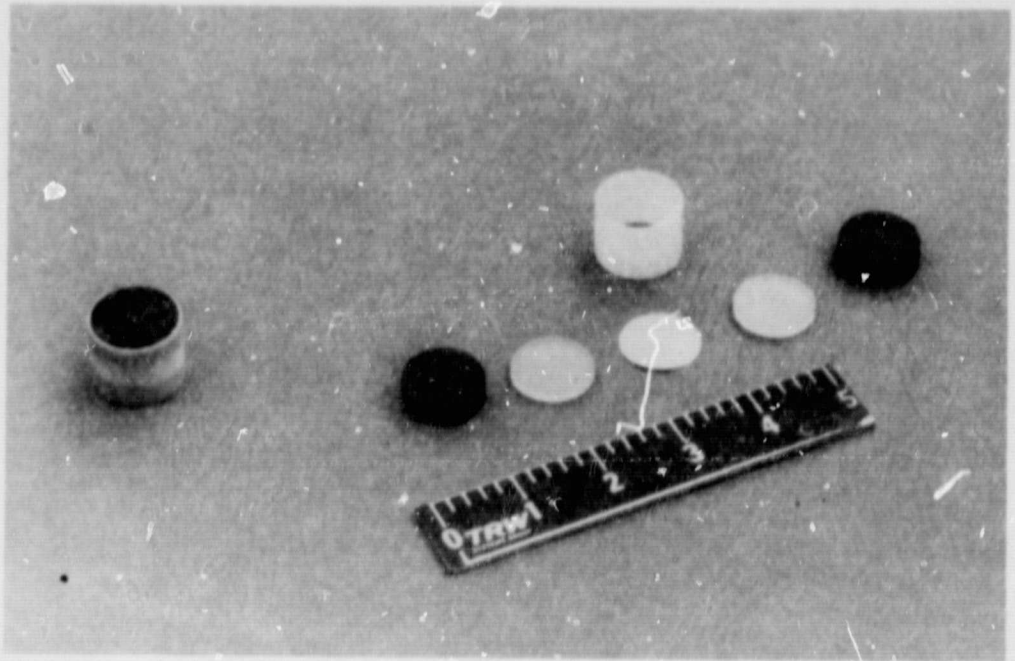
Throughout the development of circulators at TRW, computer analysis has contributed to the design of these state-of-the-art components. With circulators having been previously designed over several frequency bands, a computer program was written to more quickly arrive at a solution for a given requirement. This algorithm has grown and been revised and refined many times contributing useful information during each project. A brief discussion of the Computer Aided Design used during the switch development is contained in Section 2.4.

2.2 RF Design

The current state-of-the-art at TRW of ferrite components had its inception several years ago when a market search disclosed that the components available were inadequate by wide margins. Since that time, an impressive line of circulators has been developed over a number of waveguide bands extending well into the millimeter wave frequencies. The knowledge gained through this experience was directly applied to the design of this switching circulator. Due to the separation of RF and switching ferrites, the RF structure was initially developed as an independent unit. The rest of this section describes the RF design of a circulator with reference to a switching junction.

The circulator, which is produced at TRW, employs a cylindrical geometry which was patented in 1978. Basically, the RF section features a dual turnstile junction. As shown in Figure 2a, the circulator consists of a dielectric tube which contains two ferrite rods, two dielectric spacers, and a thin metallic wall septum separating the above parts along the center of symmetry of the waveguide to form two turnstiles. This subassembly is indexed and locked in the center of symmetry of a uniform junction of three waveguides by the metallic transformers installed in the top and bottom walls of the housing as shown in Figure 2b.

The specific design of the RF junction in the K-band switch is largely based on the typical junction configuration depicted above. There are, however, two distinctions of major significance. The thin metallic septum which was previously located in the center of a junction is now located at either end; a single dielectric disk replaces the two earlier separated dielectrics. As depicted in Figure 3, the RF junction used in a switching circulator features ferrites chamfered on the interior edge to enhance their magnetic characteristics. Dimensions for this junction are based on the non-switching junction dimensions.



137185-77

Figure 2a. Complete Set of Ferrite Junction Piece Parts

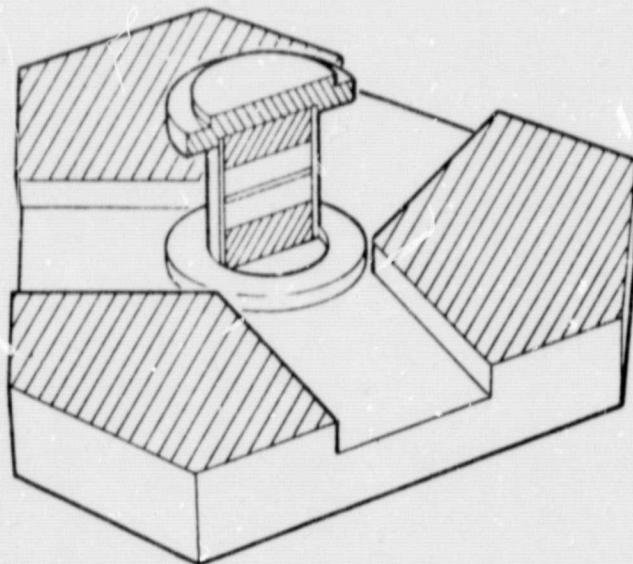


Figure 2b. Cross-Section of Circulator Showing Junction Assembly

ORIGINAL PAGE IS
OF POOR QUALITY

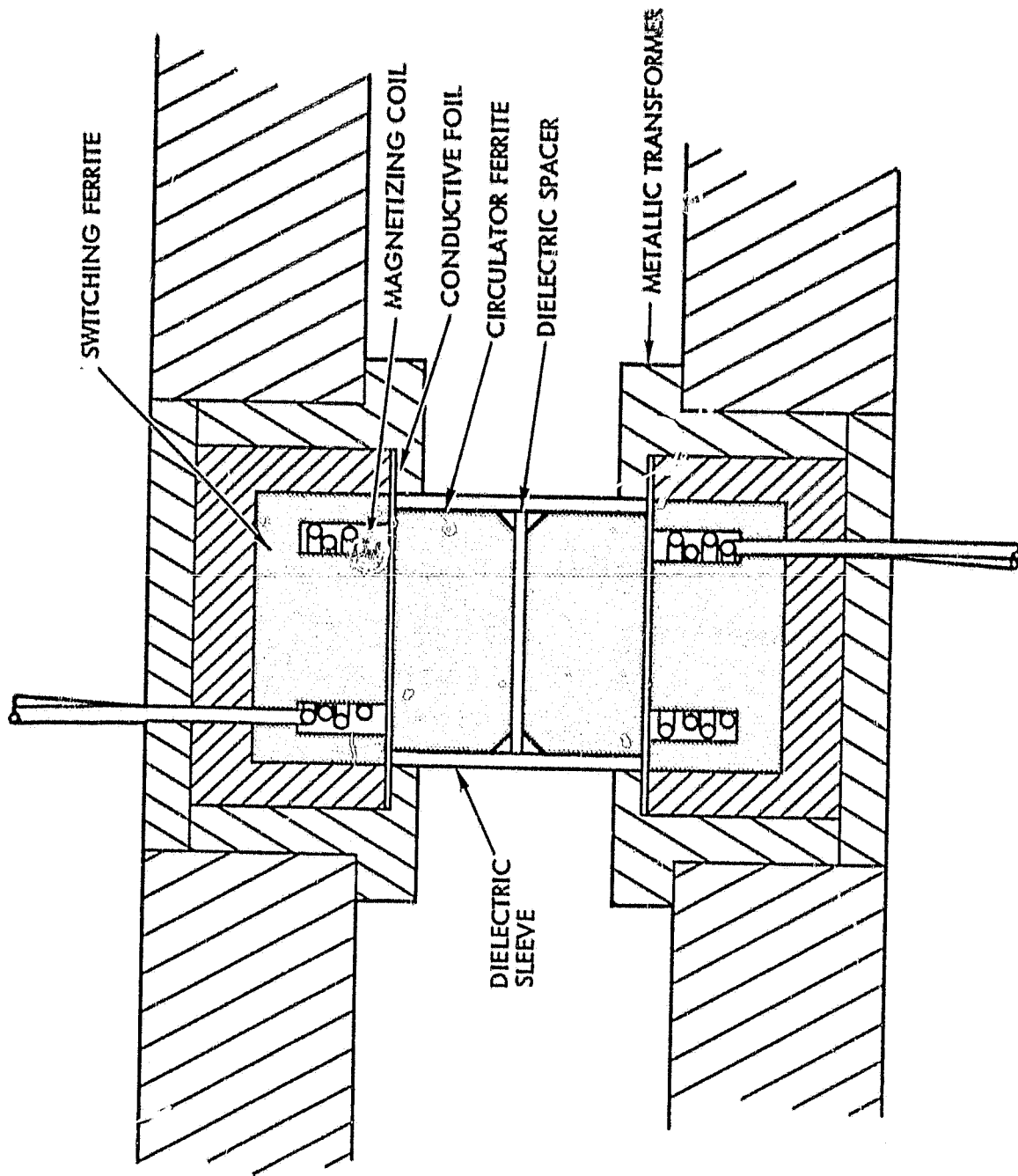


Figure 3. Cross-Section of Switching Junction Showing RF and Driver Ferrite Locations

Since a large part of the initial junction dimensions is assigned based on our computer analysis, further discussion is continued in Section 2.4. The performance of this circulator is included in Section 3.

2.3 Driver Design

The next step in the switch design process is to determine a compatible ferrite driver assembly. A driver design is based on a variety of restrictions, several of which are imposed by the RF junction dimensions. Performance is also affected by the materials and the volume of the driver.

A driver assembly is fundamentally comprised of two ferrites, one coaxially located within the other and separated by a small gap. As shown in Figure 4, this space is provided to accommodate the switching coil and to insure a high magnetic reluctance path between the ferrites. A cap of identical material is bonded to the top furnishing part of the magnetic path. Utilizing identical material in the epoxied driver, preserves the mechanical integrity as thermal expansion and vibration effects are constant throughout the unit. The RF ferrite provides for the other segment of this magnetic path depicted in Figure 5. To maintain the switch latched in its last switching condition, an intimate contact between the RF ferrites and their driver ferrites is insured by a properly designed wavy-washer spring which compresses the whole junction assembly. In this way, the thermal expansion, shock and vibration problems are effectively eliminated.

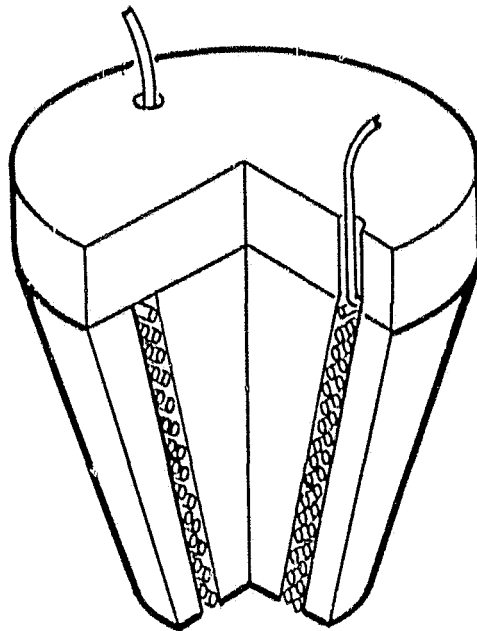


Figure 4. Driver Assembly for Switch

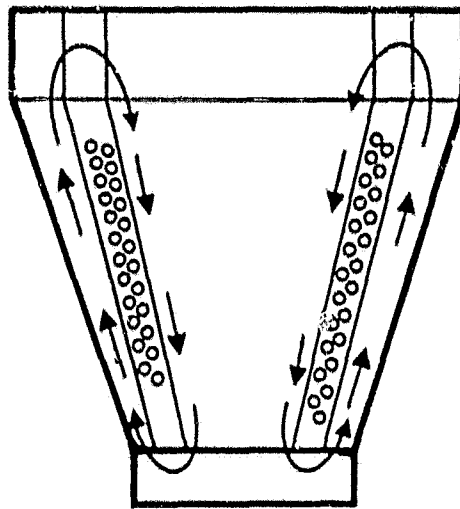


Figure 5. Magnetic Loop of Switching Junction
(Only 1/2 of Junction is Shown)

A ferrite driver has its general volume determined independently of most RF junction criteria. This is due to the fact that the size of the switching coil wire is a function of the switching current, which is essentially constant and independent of frequency. In larger waveguides, coil size is a minor problem. However, the size is a significant factor at K-band and above. It is mandatory that the ferrite driver volume remains constant; there is a minimum size required to insure the driver has adequate mass (magnetic energy storage capacity) to latch in a given direction.

The design of the RF junction significantly affects the driver design. Both the material used in the RF ferrite, as well as its shape, affect the respective elements of the driver. Ferrite used in the driver should have a high residual magnetization (B_r) with respect to the RF ferrite magnetization (B_m). A higher $B_r - B_m$ insures that the junction is properly latched. As shown in Figure 6, a magnetic hysteresis loop can be used to describe latching in the microwave switch. A driver of small $B_r - B_m$ at room temperature would be placed at point A, whereas a strongly magnetized junction would be placed at point B. A bar is sketched through each point to portray temperature effects. Notice that switch A is useless over part of its temperature range. Not only will insertion loss (among other parameters) increase significantly at greater than room temperature, but there is a possibility the junction may not latch properly at all. Use of the proper material is of major consideration when designing a switching circulator.

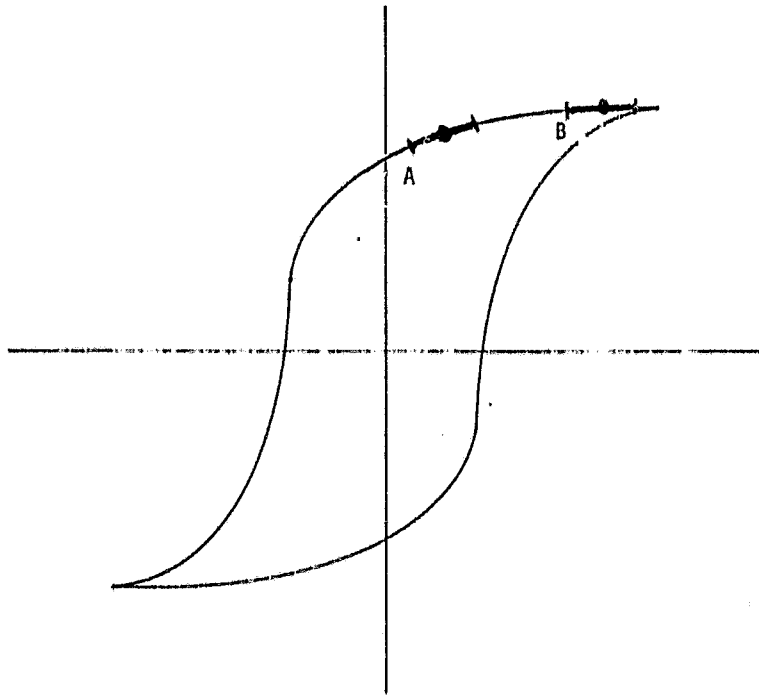


Figure 6. Hysteresis Loop of Switch with Two Sets of Drivers
 A: Low $B_r - B_m$; B: Higher $B_r - B_m$

Another less pronounced effect is related to the diameter of the RF ferrite. Previous experience has shown that at the interface between the RF and driver ferrite, the driver has certain limits on its diameter. The actual size of the driver is determined during the breadboard development.

2.4 Computer Aided Design

As noted in earlier sections of this report, computer aided design has played an increasing role in the development of non-switching junction circulators. Each component part of a junction interacts to form a complete circulator and is the basis of the algorithm which is discussed below.

Primary considerations for any circulator design program are the ferrite characteristics. The most important parameters are the ferrites' dielectric constant and saturation magnetization. Analysis of this dielectric constant with respect to frequency yields important information about the size of the ferrite. The ferrite length and diameter are also governed in part by the R/L ratio and operating modes. Saturation magnetization likewise affects the ferrite dimensions, but not as acutely as the dielectric constant.

Determination of the other component dimensions extends from the ferrite dimensions. Again, dielectric constant is of importance in the spacer and containment tube. Waveguide size has a predominant influence on the lengths of these impedance matching elements. An extensive algorithm is devoted to calculating junction components once ferrite dimensions are determined. Sample output for a circulator designed at X-band is shown in Figure 7.

Design of a non-switching circulator employing the aid of a computer has been recently expanded to include switching circulators. A discussion of these refined programs is included in Section 3.4, Switch Development.

 WAVEGUIDE JUNCTION CIRCULATOR DESIGN DATA

INPUT DATA

```

-----
FREQUENCY RANGE (GHZ) ?      10
FREQUENCY INCREMENT (MHZ) 1500
SATURATION MAGNETIZATION (GAUSS) 1600
WAVEGUIDE HEIGHT (IN) 0.497
FERRITE DIELECTRIC CONSTANT 15.1
SPACER DIELECTRIC CONSTANT 2.57
G EFFECTIVE 1.93
  
```

JUNCTION DESIGN PARAMETERS

```

-----
F(GHZ)      L(IN)      MS      MU      E      ZC/Z0
-----
7.0000     1.6861     0.6236     0.5986     3.2217     0.2459
8.5000     1.3886     0.5218     0.7277     5.5760     0.3997
10.0000    1.1803     0.4435     0.8033     4.0286     0.5813
  
```

JUNCTION DIMENSIONS

```

-----
F(GHZ)      LD(IN)      D(IN)      HTN(IN)      HY(TN)      T(IN)
-----
7.0000     0.0249     1.1711     0.5641     0.2464     0.1252
8.5000     0.0647     1.0223     0.5685     0.3142     0.0914
10.0000    0.1550     0.9181     0.7083     0.3789     0.0590
  
```

Figure 7. Sample Output of Circulator Design Program

3. SWITCH DEVELOPMENT

3.1 Introduction

Development of the K-band latching switch was broken into several projects of varying emphasis. Prior to development, a reflectometer test set was assembled, calibrated, and tested. Breadboard activity proceeds with the fabrication and tuning of a fixed junction circulator. Once the circulator is finished, development is extended to the actual switch requiring the longest period of effort. The final development stages of the switch are paralleled by the design and fabrication of the switch actuating circuitry. These activities are discussed in this part of the report, as well as presentation of the final results. Section 3 concludes with the results obtained from shock and vibration tests and measured thermal characteristics.

3.2 Instrumentation

Development of a latching switch at K-band requires a properly calibrated test circuit and instruments. Since a microwave source that operates from 15 to 22 GHz is not readily available on the market, a K-band circuit which operates from 18 to 26.5 GHz was substituted. This waveguide latching switch design was intended for frequencies from 18 to 20 GHz, which allows the substitution. Transitions from the WR-42 waveguide employed in the test bench, to WR-51 required for the switch, are utilized where necessary to accommodate the switch and detector isolator. Figure 8 contains a schematic of the microwave circuit used for this project. In this circuit, there are two components which can create erroneous measurements if inaccurately manufactured - the load and the detector. Testing and tuning of these units is necessary to obtain reliable results.

The basic instrument to measure power is a crystal detector and should, therefore, be a perfect load to prevent reflections. Any mismatch in the unit would visibly degrade the true performance of any component under investigation. Unfortunately, most commercial detectors present some mismatch to a microwave circuit, as shown in Figure 9a. Inserting an attenuator prior to the detector enhances VSWR (Figure 9b). This type of tuning is used in the VSWR detector of Figure 8, where the 10 dB directional coupler duals as an attenuator. However, an attenuator pad is not as useful as an isolator for the following reasons: 1) there is a significant improvement in isolation, and 2) more power is transmitted to the detector with an isolator. A combination of the attenuator and isolator results in an acceptable impedance match, as shown in Figure 9c. Tuning of the detectors effectively prevents impedance mismatch at the instrument from degrading the entire circuit.

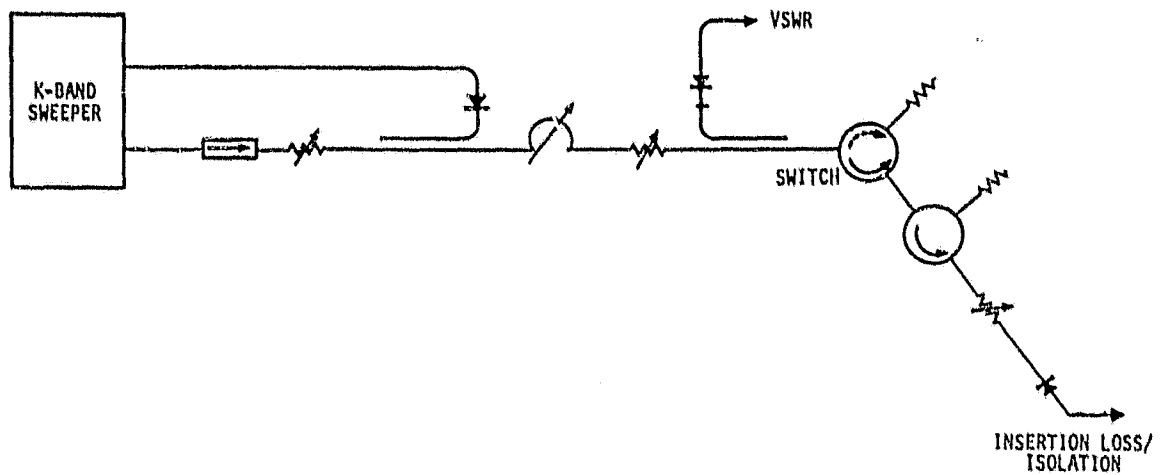
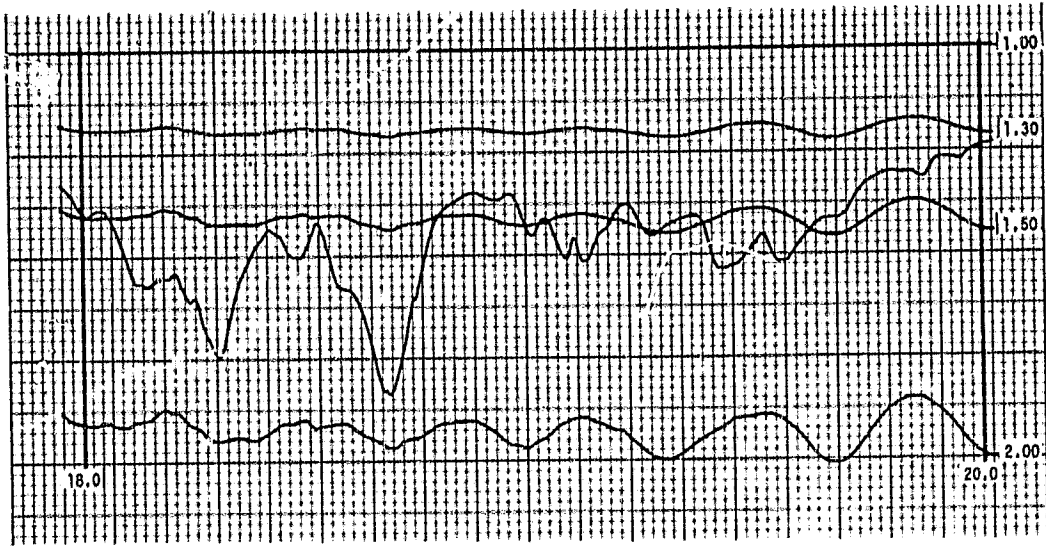


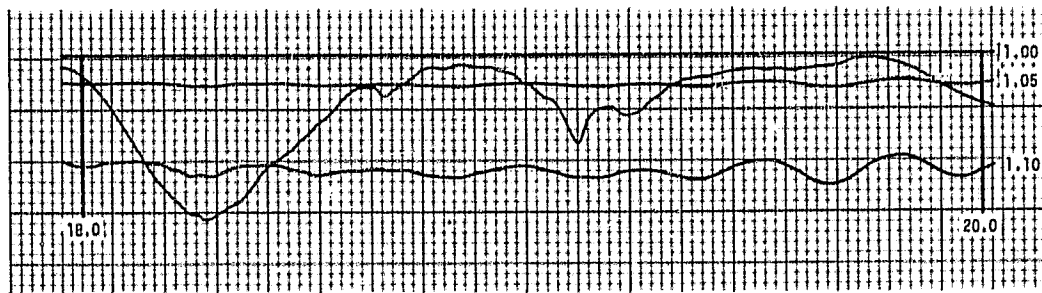
Figure 8. Schematic of K-band Development Circuit

Another component which can adversely affect component measurements is a load. Similar to the detector, a load may reflect a portion of its input power, thereby affecting the performance of the test unit. Figure 10 dramatically illustrates the effect a poorly assembled load has on the performance of an adjoining circulator. Examining the available loads, it was determined that commercial K-band loads were inadequate. Consequently, we designed and constructed loads at our laboratory. Typical performance of the WR-51 loads is depicted in Figure 11.

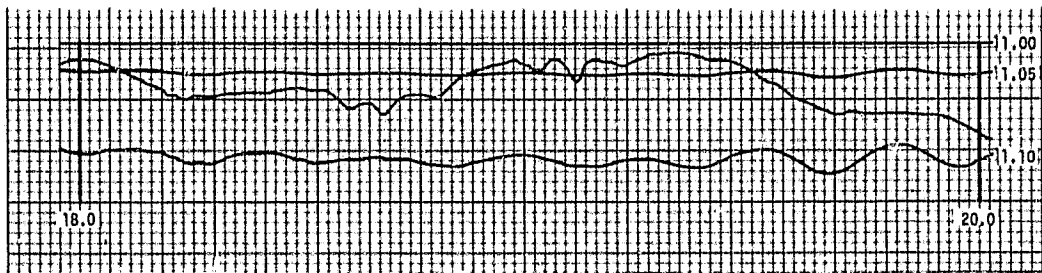
One final consideration in our measurement bench is the isolating circulator. Throughout the development of our own fixed junction circulator, another available non-TRW circulator was utilized. Upon completion of the fixed junction, our superior circulator design in WR-51 replaced the test bench WR-42 circulator, which also eliminates any waveguide mismatch (Figure 8). Periodic tests insured system integrity throughout the duration of the project.



a.



b.



c.

Figure 9. VSWR of Detector
 a. Detector only
 b. Detector with attenuator
 c. Detector with isolator
 and attenuator

RECEIVED
 AIR FORCE
 RESEARCH
 LABORATORY
 WRIGHT-PATTERSON
 AIR FORCE BASE
 DAYTON, OHIO

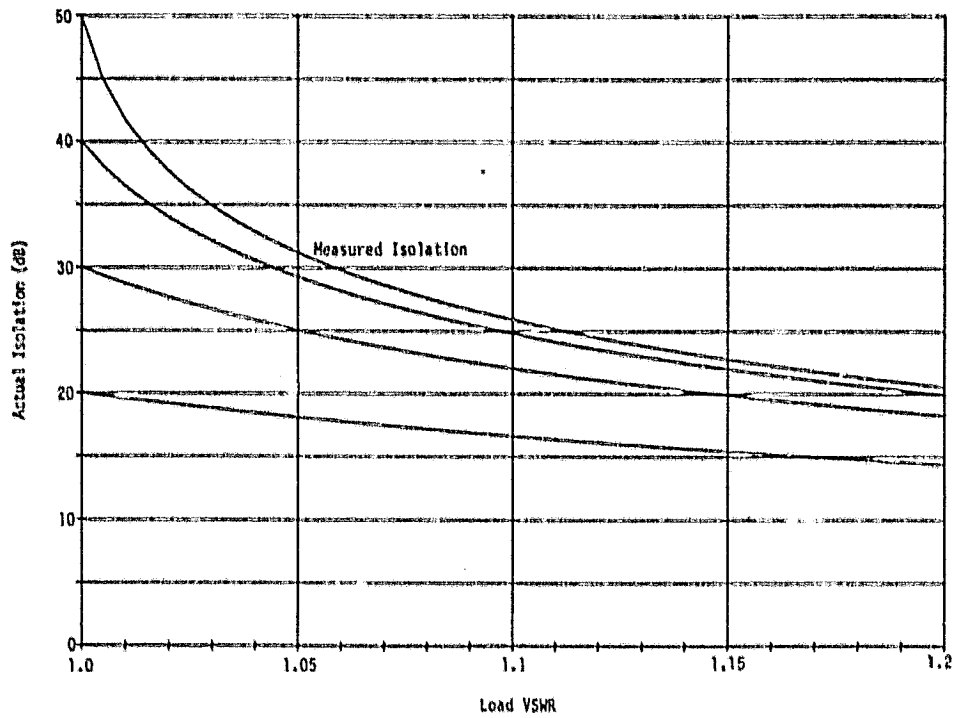


Figure 10. Degradation of Circulator Isolation with Load VSWR

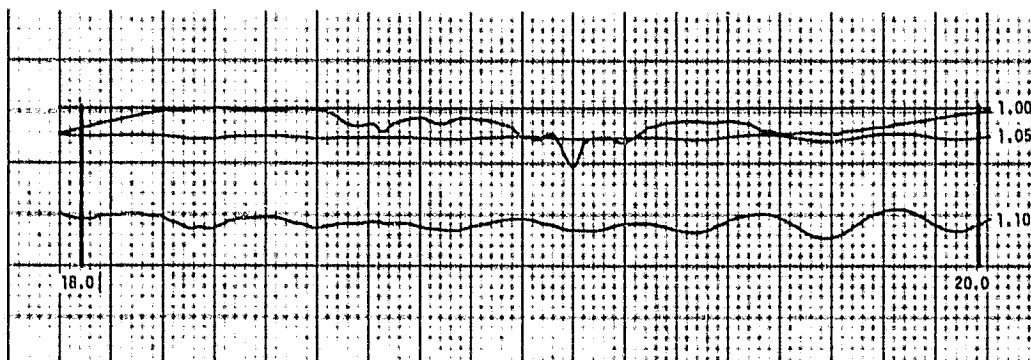


Figure 11. VSWR of TRW Load

3.3 Fixed Junction Circulator

The design of a K-band non-switching circulator was established from efforts on circulators at other frequencies and results from our computer program. As described in Section 2.4, this program generated initial junction dimensions from which bread-board development ensued. The unit is fine-tuned to provide a junction with excellent performance from 18 to 20 GHz.

With material procurement completed by June of 1979, the non-switching junction was constructed. Initial development began with TT2-4000 ferrites; analysis throughout the first phase continually assured us that this was the proper material. The ferrite and other junction materials were fabricated according to the dimensions suggested by computer analysis which are shown normalized in column A of Table 2. After several weeks of fine tuning, the performance of the non-switching junction was optimized over the desired band. Final dimensions for this circulator are included in column B of Table 2, normalized to the computed dimensions.

The non-switching circulator served two purposes for the development of a switching junction at K-band. First, it provides the initial dimensions for the RF junction ferrites of the switching junction. Previous efforts have indicated that reasonable initial dimensions for the switching junction are related to the fixed junction results. Also, the junction was utilized as a fine-tuned isolator to enhance the measurement accuracy of our test bench as discussed in the previous section. Performance data on this circulator is presented in Figure 12.

Table 2. Normalized Comparison of Non-Switching Junction Dimensions
A. Computer Analysis; B. Actual

Variable	Definition	A	B
D_f	Ferrite Diameter	1.00	0.98
L_f	Ferrite Length	1.00	1.08
L_d	Spacer Length	1.00	0.88
t	Transformer Height	1.00	0.86
D	Transformer Diameter	1.00	1.02

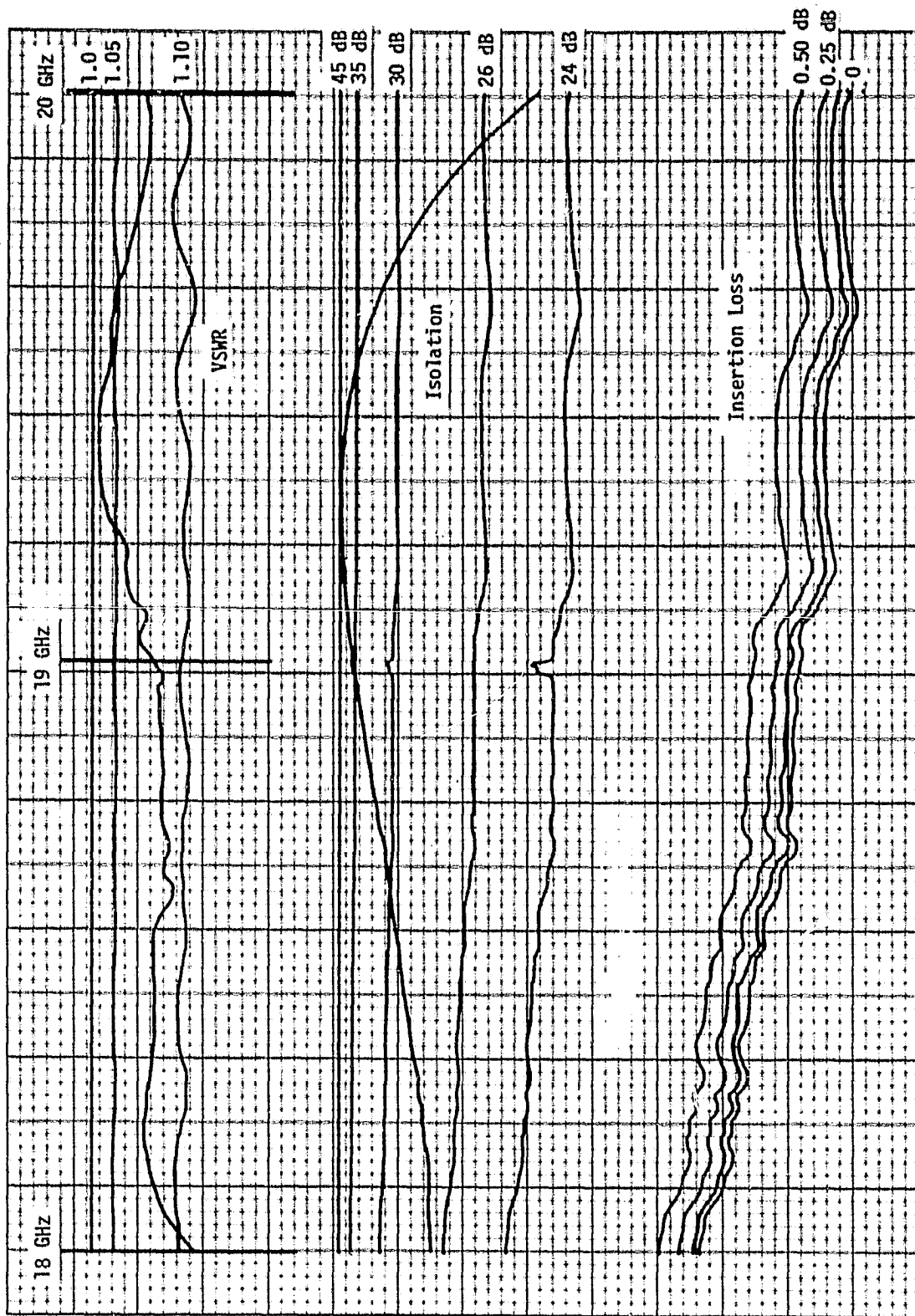


Figure 12. Final Performance of Non-Switching K-Band Circulator

3.4 Latching Switch Development

The K-band latching switch development began with the assembly of a junction with dimensions calculated from the fixed junction size and ferrite driver restrictions. Since this particular band does not boast a microwave latching switch with such excellent characteristics, development also involves learning and understanding the particular limits of this project. The completed switch advances the state-of-the-art of microwave devices. A presentation of the actual development is included in this section of the report.

Early in the extension of a latching switch from X-band to K-band, a housing design was chosen. Principal considerations are waveguide path and size; there is electrically a very short path through the junction to minimize guide losses. Miter corners allow a low loss bend from the necessary 120° junction angle to the desirable 90° angles for a simplified circuit connection. Another detail concerns the housing dimensions. The switch should be as compact as possible while ensuring that it is still capable of housing the driver ferrites and actuating circuitry. This design is shown in Figure 13.

After the housing design was completed, analysis of ferrites to select the proper materials was initiated. Use of TT2-4000 in the non-switching junction made this the first choice for the switch. Evaluation continued throughout the project with C-11 and C-44 also showing promising results. The TT2-4000 ferrite was selected due to its superior performance over the desired frequency range.

Choice of the RF ferrite has a direct influence upon the driver material which can be used. Originally, TT6-2800 was determined to be adequate for our needs. Later development disclosed that TT71-4100 was superior to TT6-2800. The reasons for selecting this material were presented in Section 2.3.

The ferrites and dielectric used in the switch were under continued evaluation to verify compliance with material standards and specifications. Other parts, such as the housing and transformer, were inspected to insure all parts are within tolerance. Quality control for the K-band switch was similar to the system used for the fully space qualified DSCS II, Phase 2 and Landsat latching switch.

As discussed earlier in Section 2, the non-switching junction results are utilized in the switching junction design. Essentially, the ferrite dimensions are expanded to accommodate the magnetic return path which allows a switching junction to operate properly. Other component parts are adjusted accordingly for impedance matching.

The first latching switch (designated -1) was completed in early August. Its performance was satisfactory, although it did not meet all of the program requirements. Figure 14 shows the performance of this switch. Note that the only objective not reached was bandwidth; this particular unit was 100 MHz short of the 1400 MHz required. Other requirements were successfully obtained.

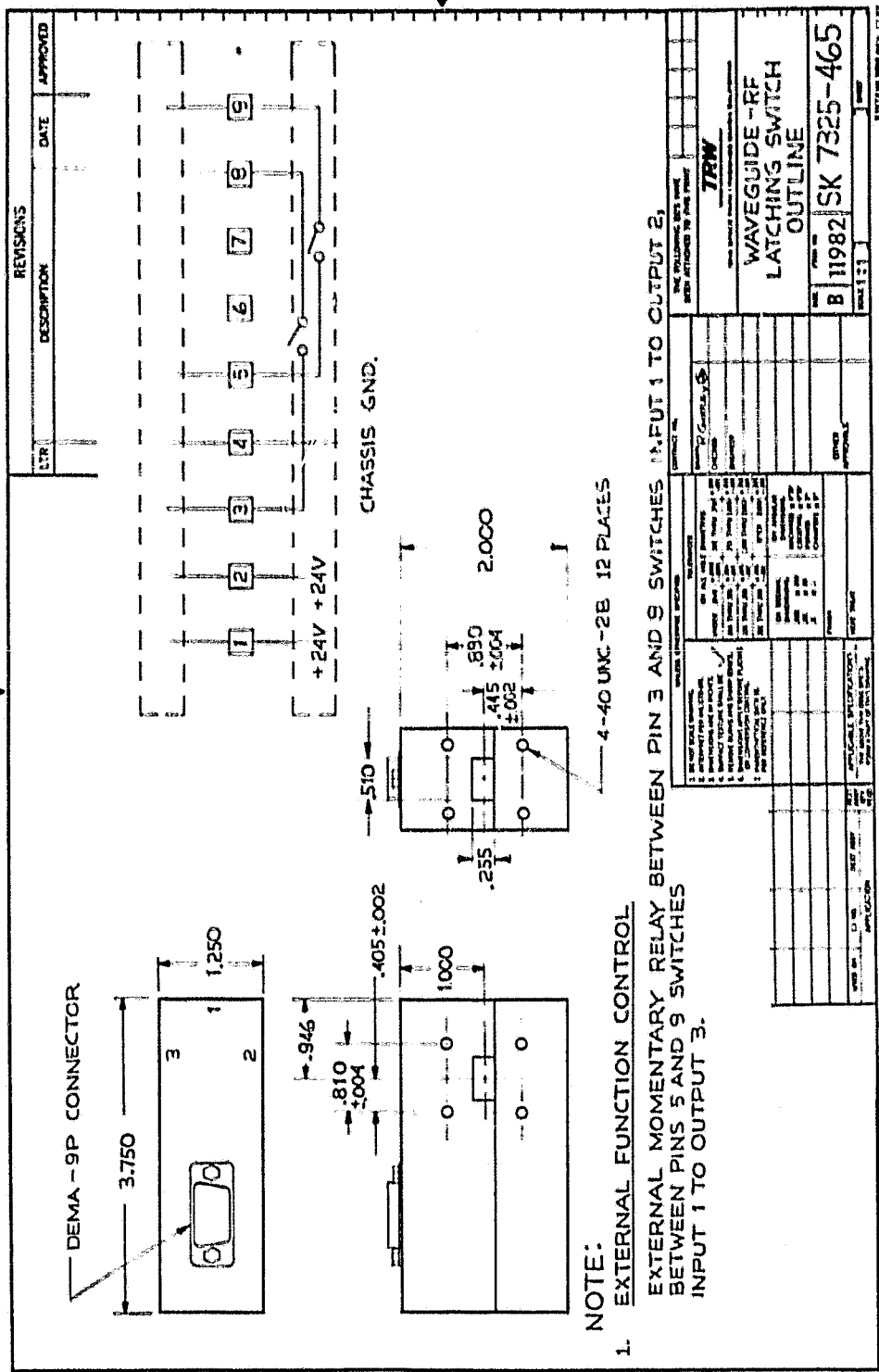


Figure 13. Housing Design for K-Band Switch

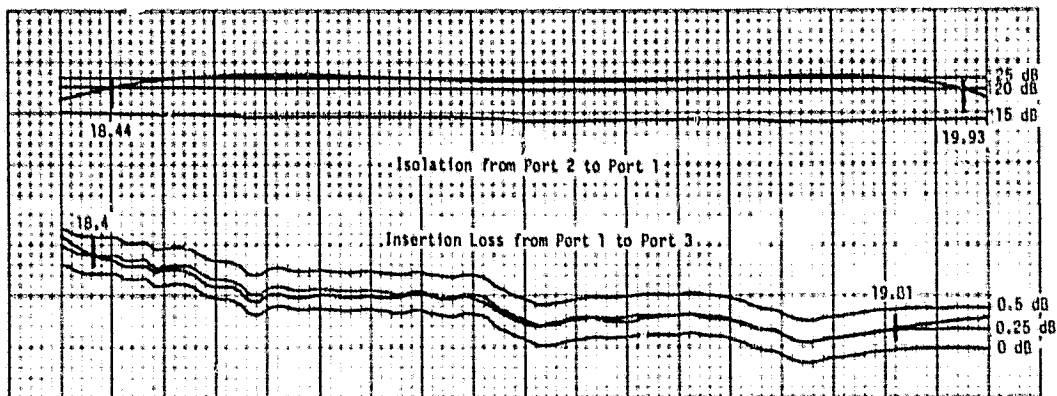
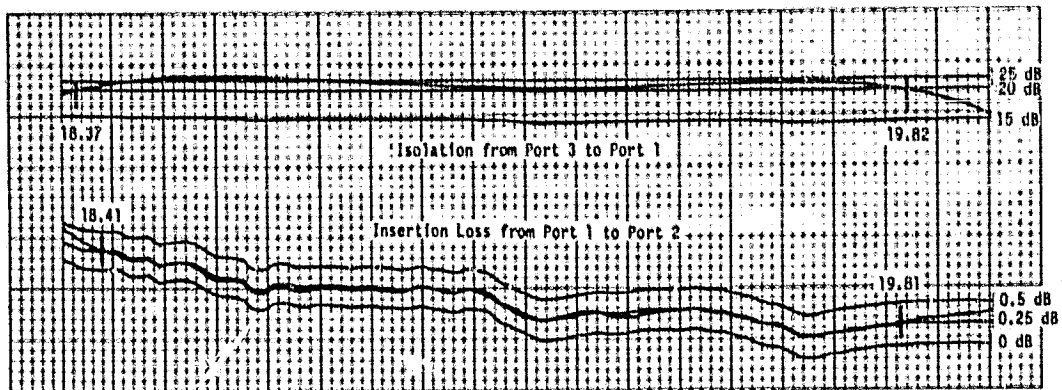
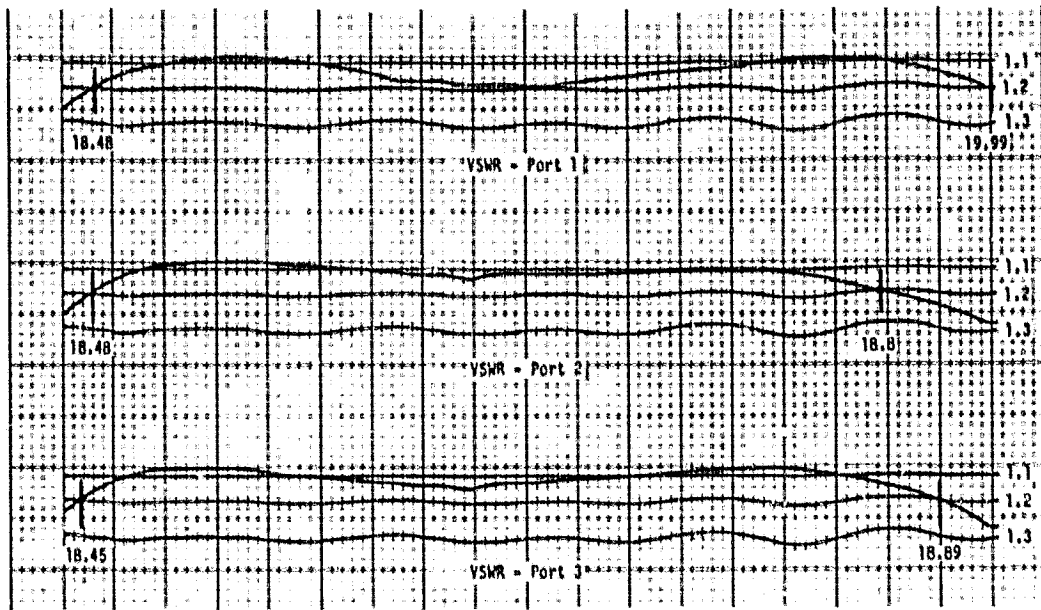


Figure 14. Final Performance of K-band Latching Switch (-1)

With the first unit completed, a second unit was assembled and further refinements were made. The modified switch exhibited an improvement in bandwidth, as well as isolation. The performance presented in Figure 15, as well as the data contained in Table 1 on page 1-2, clearly show the improvement. Our second unit successfully met all of the project requirements.

Although the switches were designed individually and do not exhibit the same performance, all other specifications are identical. Table 3 contains all data pertinent to a designer in order to interface the switch with other components.

Table 3. Interface Data for K-Band Switch

Item	Description
Weight	355 g (12.5 oz.)
Size	9.53 cm. x 3.18 cm. x 5 cm. high (3.75 in. x 1.25 in. x 2 in. high) (See Figure 13, page 18)
Waveguide	WR-51
Flange	WR-51 Cover
External Connector	DEMA-9P (See Figure 13, page 18 and Figure 16, page 18 for wiring)
Power Supply	24-28 Vdc Maximum current required (during switching only) 1 mA
Switching Time	50 μ sec
Max. Power Input	100 W (CW)

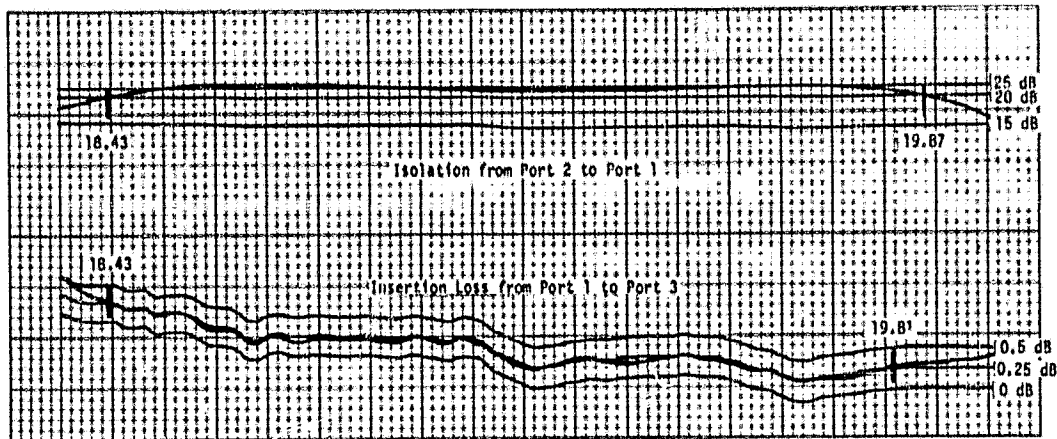
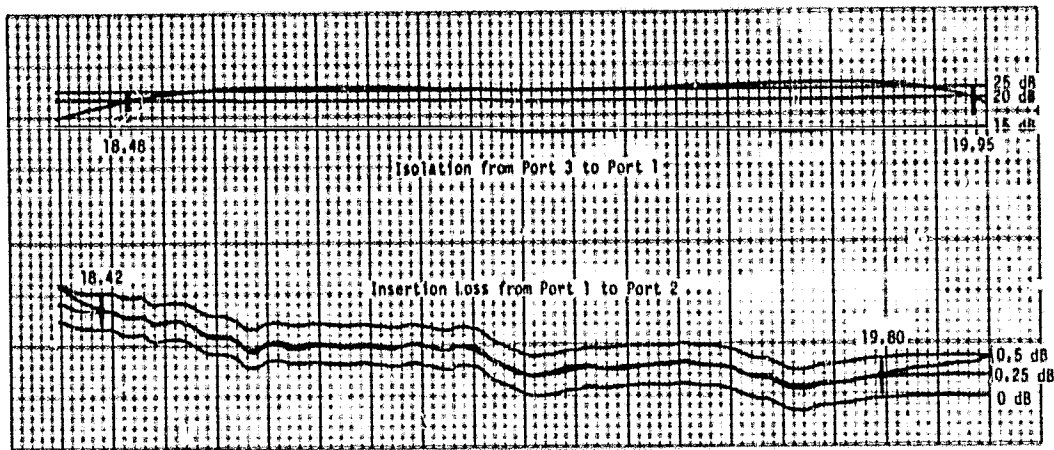
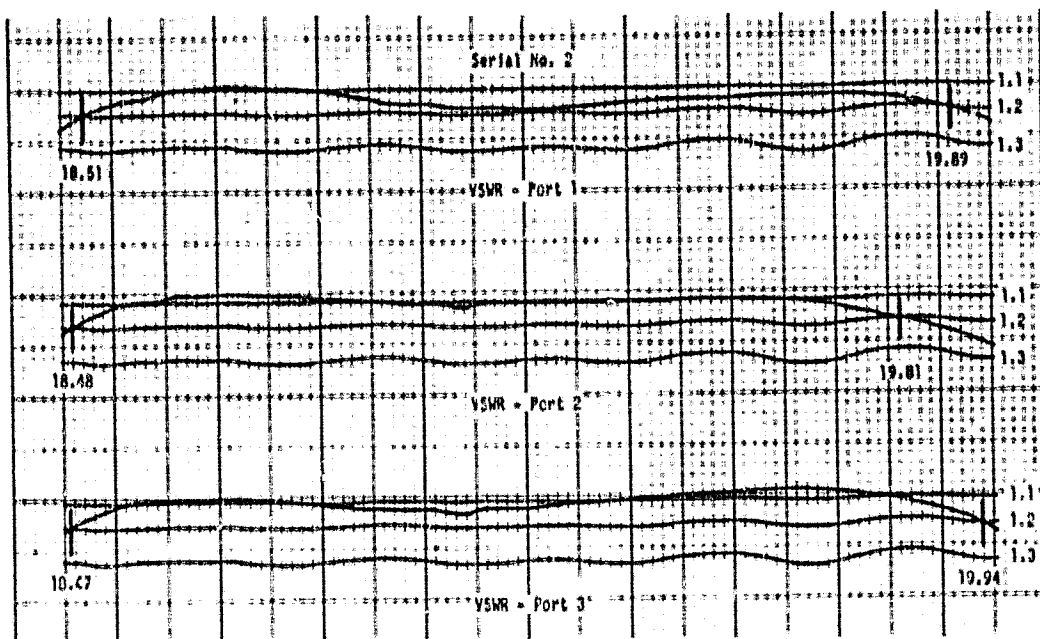


Figure 15. Final Performance of K-Band Latching Switch (-2)

3.5 Switch Actuating Circuitry

The size of the K-band switching housing is dictated in part by the actuating circuitry which is contained inside the unit. All that is necessary to operate the switch is an external 24 volt power supply and two SPST switches. Closing one external switch will activate the unit for clockwise circulation, while the other switch will activate the unit in the opposite direction. Switching time is approximately 50 μ sec with a recharge period of 30 seconds necessary between successive actuations of the same circulation direction.

The schematic for the latching switch actuating electronics consists of two independent circuits, one for each direction of circulation. Each driver has two adjacent coils built into the driver which are electrically independent. As shown in Figure 16, one driver contains coils 1A and 2A, while the other contains 1B and 2B. Each circuit has its own bank of discharge capacitors, series dropping resistor, and trickle charge resistor. A series dropping resistor limits current in the devices during capacitive discharge. Similarly, a trickle charge resistor limits power supply requirements for charging and prevents excessive loading on either the supply or K-band switch coils should a SPST breaker become frozen in the closed position. The pin assignment used for the 9 pin D connector is also included in the figure.

Though the actuation circuitry for the latching switch has two independent circuits, they are combined onto a single board. This board is designed such that each side holds the components for an entire circuit as displayed in Figure 17. Note that each side contains four capacitors to increase reliability; switching capability is still intact with two capacitors disconnected. The circuit board is placed into a cavity located inside the switch housing. Special foam is packed around the board enabling the unit to pass shock and vibration requirements with ease. Figure 18 shows a hidden view of the board as it resides in the latching switch.

The power supply for the switch should be at least 24 volts. Switching will still occur reliably at 15 volts, but the recovery time for the actuating circuitry is longer.

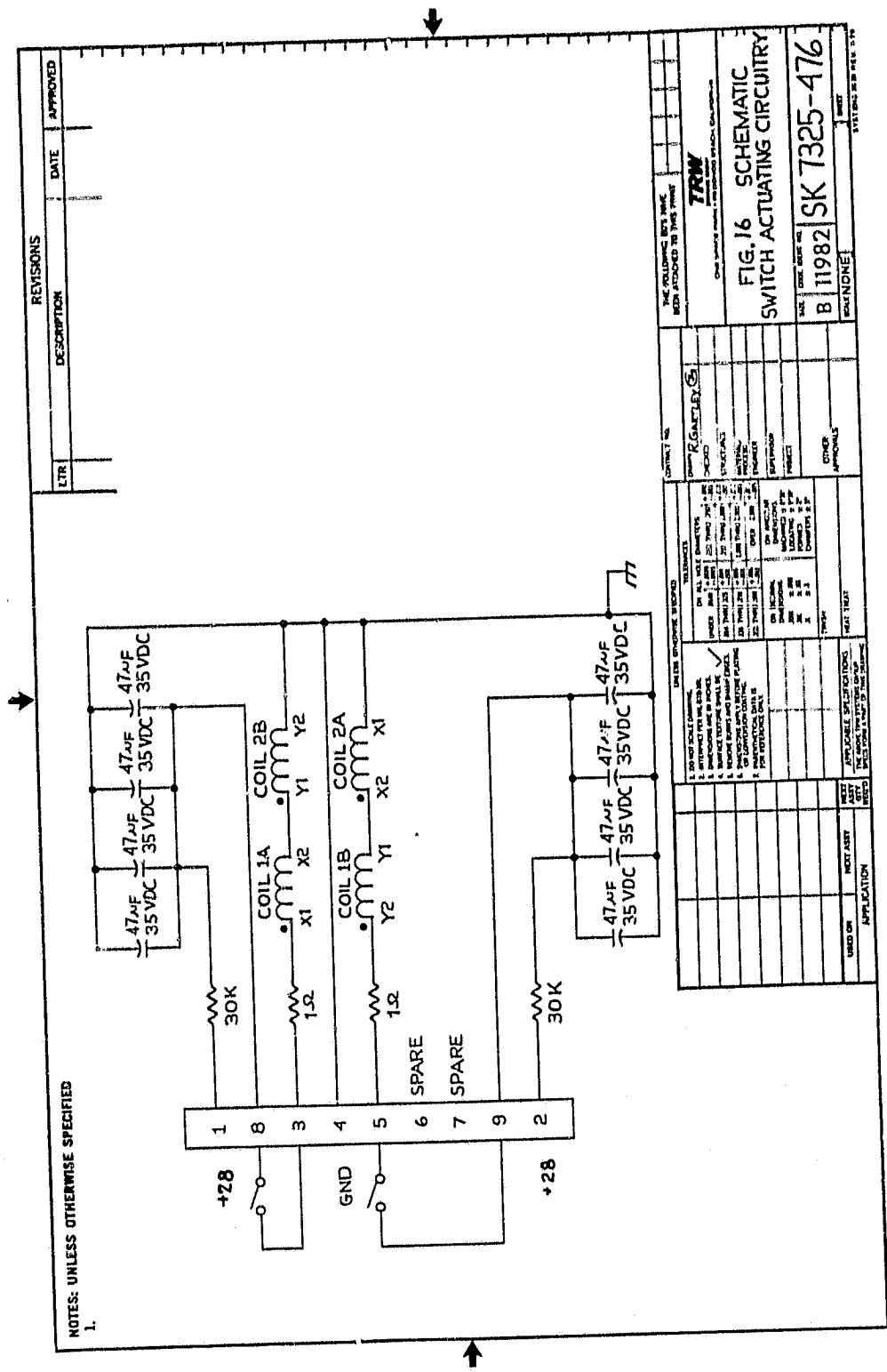


Figure 16. Schematic of Latching Switch Actuating Circuitry

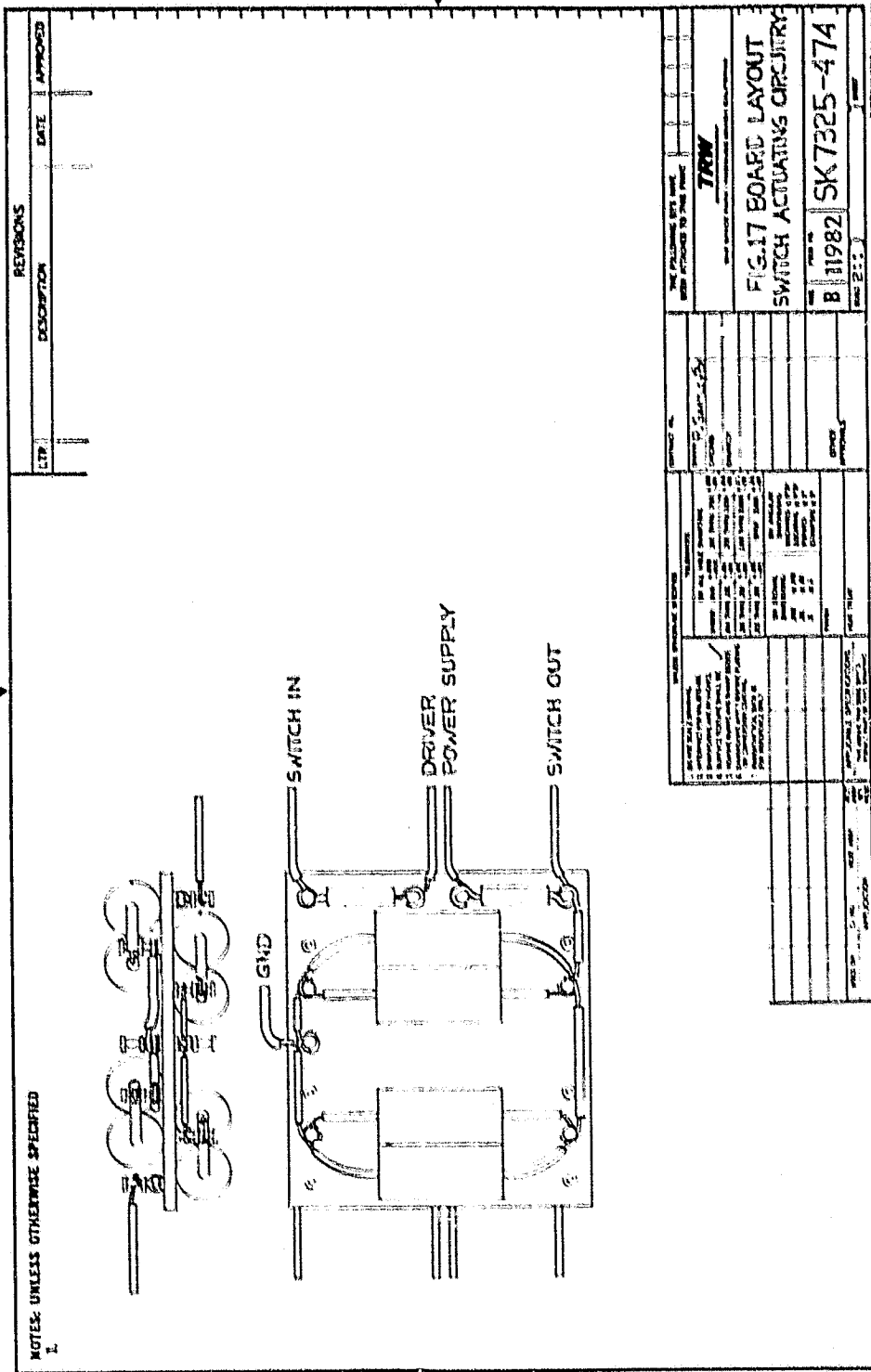


Figure 17. Board Layout of Switch Actuating Circuitry

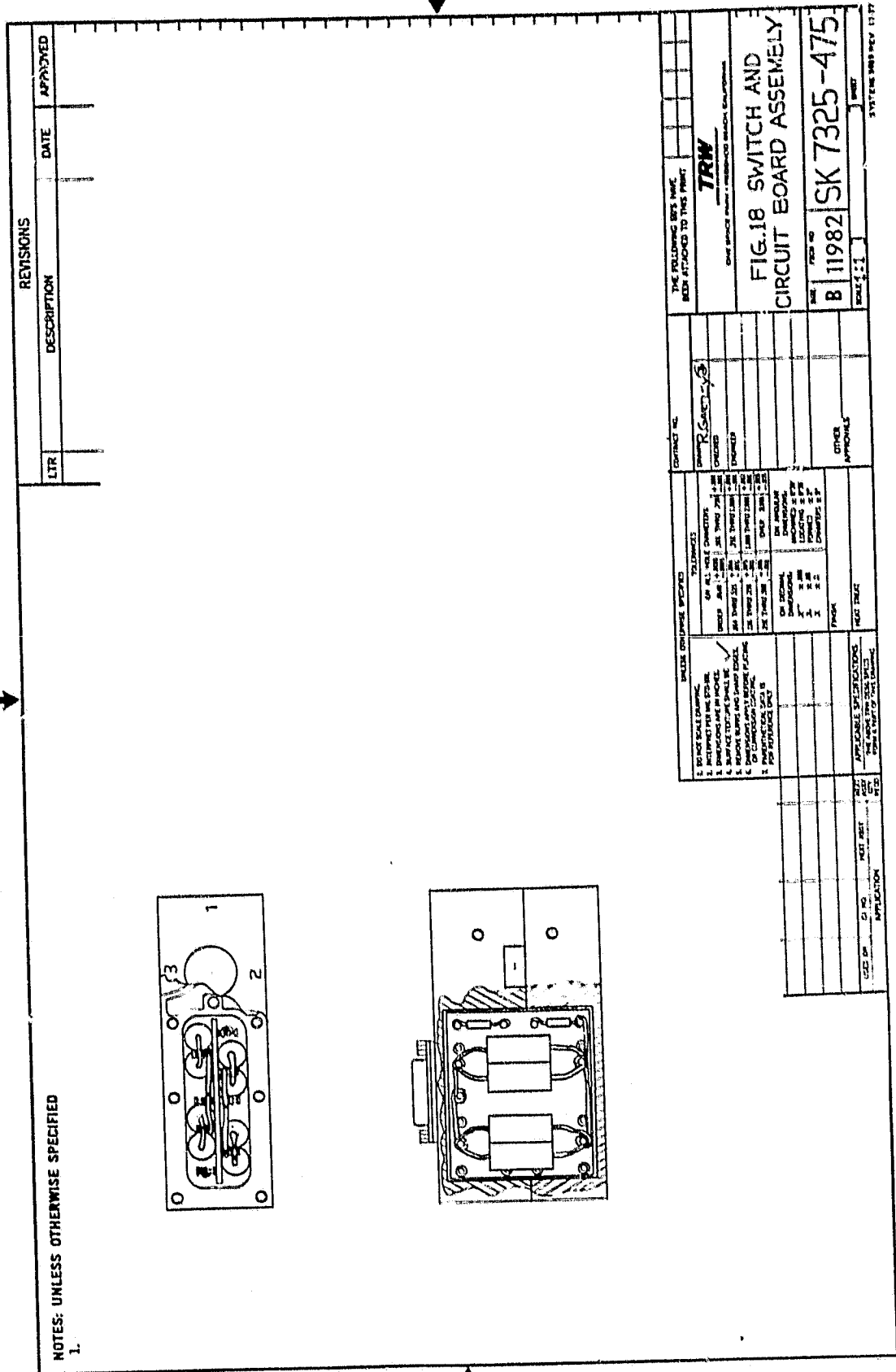


Figure 18. Internal View of Actuating Board

3.6 Shock and Vibration

After completing the second latching switch, this unit was sent to the Environmental Test Department for shock and vibration tests. The results of this testing apply to both K-band units as the mechanical design is identical. (Small changes in the junction dimensions do not affect the structure of the switch.)

The testing of our -2 K-band switch followed the test procedure dated 6 November 1979. This procedure outlines the type and level of both the shock and vibration tests. Specific documents which form a part of this procedure are NAS3-21761, provided by NASA, and EV2-48 generated by TRW. A summary of the shock and vibration guidelines is contained in Table 4.

Table 4. Shock and Vibration Test Program

Ambient Condition:

Temperature	65-80°F
Relative Humidity	70% RH or less
Barometric Pressure	between 28 and 32 inches of mercury

Vibration:

Perpendicular to mounting surface

<u>Frequency</u>	<u>Level</u>
200-100 Hz	Increase at 6 dB/octave to $0.4 \text{ g}^2/\text{Hz}$
100-180 Hz	$0.4 \text{ g}^2/\text{Hz}$
180-1000 Hz	$0.3 \text{ g}^2/\text{Hz}$
1000-2000 Hz	Decrease at 6 dB/octave
Overall grms = 21.01	

Parallel to mounting surface

<u>Frequency</u>	<u>Level</u>
20-100 Hz	Increase at 6 dB/octave to $0.1 \text{ g}^2/\text{Hz}$
100-1000 Hz	$0.1 \text{ g}^2/\text{Hz}$
1000-2000 Hz	Decrease at 6 dB/octave
Overall grms = 11.97	
Test duration	One minute per axis for each of three orthogonal axes

Shock:

Amplitude	30 "g's"
Duration	8 mS
Test to be done on all three axes	

As noted in the original test program, the switch performance is measured prior to each test and again after test completion. Final performance of the switch is recorded before the vibration test; this data was shown in Figure 15. Vibration tests were consistent with the guidelines contained in Table 4. Figure 19 shows the results of the vibration tests for all three axes of the switch.

Referring to Figure 13, which shows the housing design, the X-axis is perpendicular to the port 1 flange. A line which is perpendicular to the port 2 flange (or port 3) is the Y-axis, with the Z-axis perpendicular to the top surface of the switch.

After vibration tests are completed, the switch performance is compared to its original data, indicating latching has been maintained. The switch is then returned to environmental test to obtain shock data; results for this test are shown in Figure 20.

A final set of measurements is taken on the -2 K-band switch performance after shock tests are complete. The status of the switch is closely monitored to verify that the unit is still positively latched. Comparison between the original measurements and this final set will reveal any flaws in the switch design. The post-shock data used for comparison is presented in Figure 21.

An examination of the final performance of the K-band switch shows negligible change in performance. Both shock and vibration tests were passed without difficulty. The switch remained latched in its last position throughout either test without any degradation in performance; it is clear that the switch is mechanically and electrically qualified for the rigors of space.

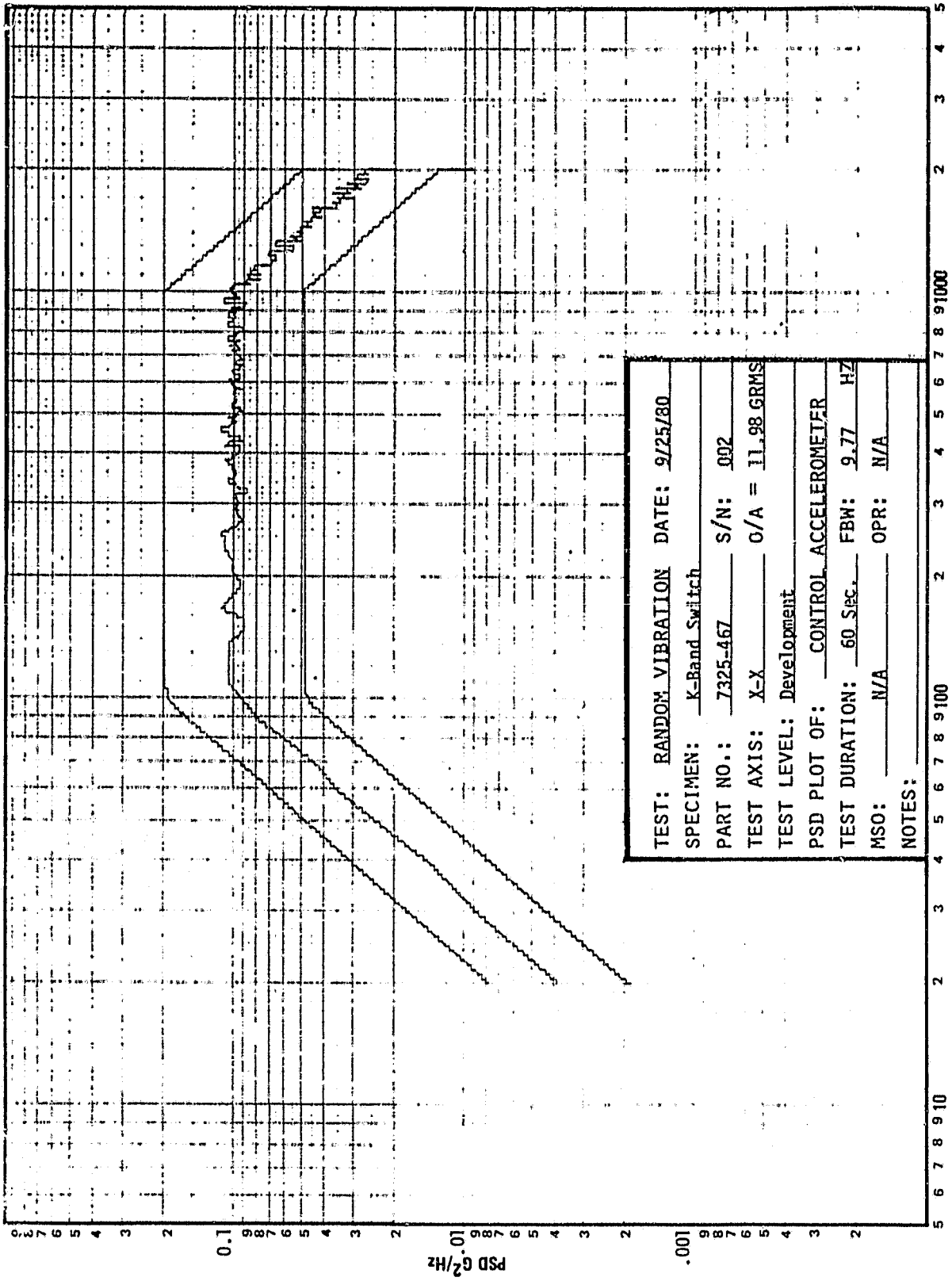


Figure 19a. K-band Switch Vibration Test Data: X-Axis

ON PAGE 1
OF 200

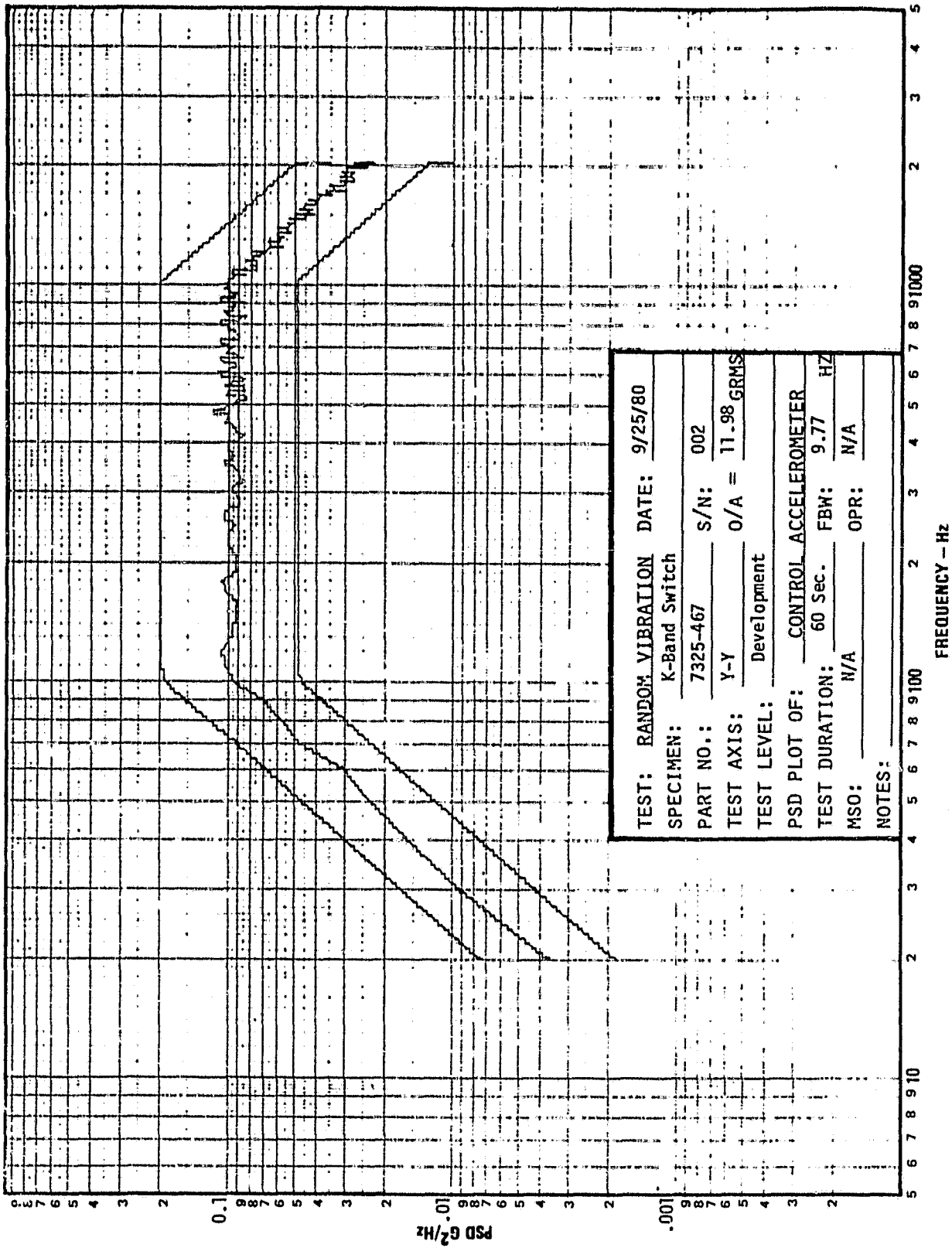


Figure 19b. K-Band Switch Vibration Test Data: Y-Axis

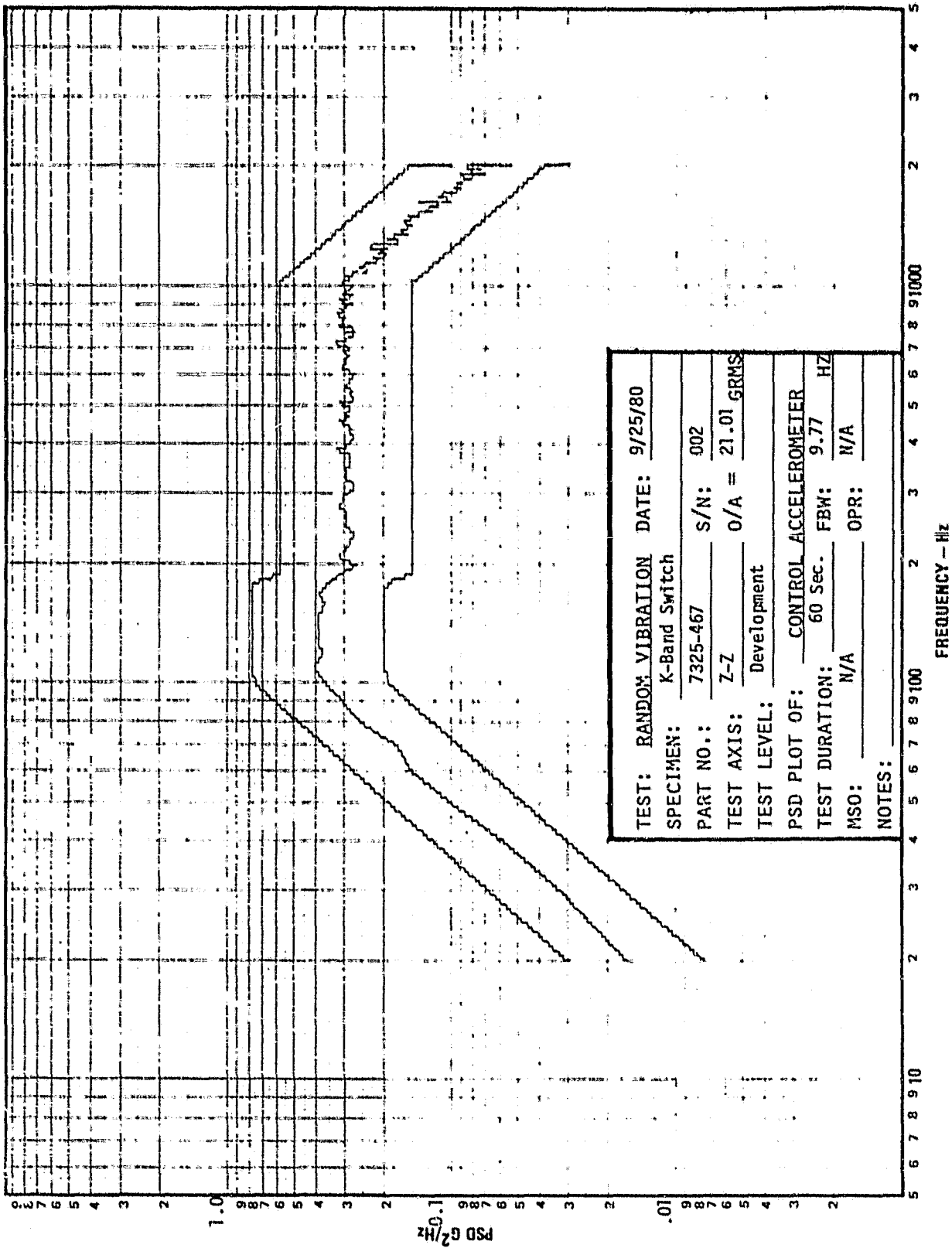


Figure 19c. K-Band Switch Vibration Test Data: Z-Axis

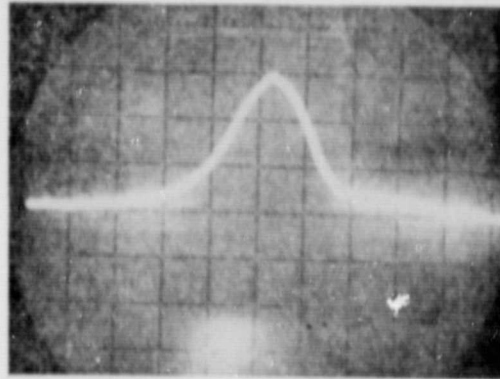
ORIGINAL PAGE IS
OF POOR QUALITY

UNIT: K-Band Switch
S/N: 002
CALIBRATION
Vertical: 10 gpk/cm
Horizontal: 2 ms/cm

AXIS: +X

ACCEL: Control

PULSE: 1

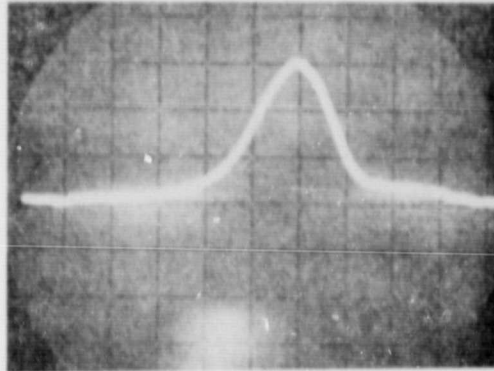


UNIT: K-Band Switch
S/N: 002
CALIBRATION
Vertical: 10 gpk/cm
Horizontal: 2 ms/cm

AXIS: +X

ACCEL: Control

PULSE: 2



UNIT: K-Band Switch
S/N: 002
CALIBRATION
Vertical: 10 gpk/cm
Horizontal: 2 ms/cm

AXIS: +X

ACCEL: Control

PULSE: 3

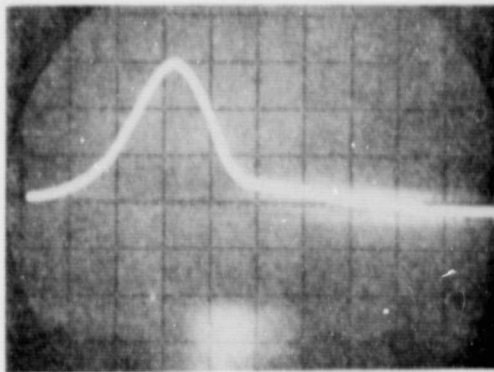
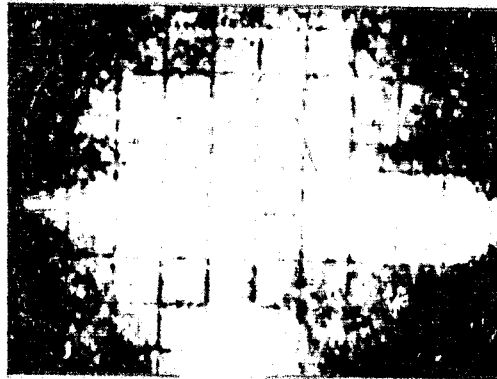
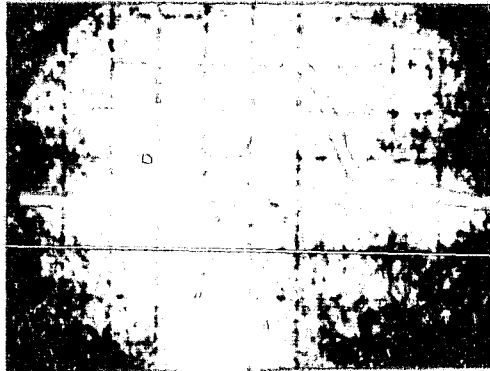


Figure 20a. K-Band Switch Shock Test Data: +X Axis

UNIT: K-Band Switch
S/N: 002
CALIBRATION
Vertical: 10 gpk/cm
Horizontal: 2 ms/cm
AXIS: +X
ACCEL: Control
PULSE: 1



UNIT: K-Band Switch
S/N: 002
CALIBRATION
Vertical: 10 gpk/cm
Horizontal: 2 ms/cm
AXIS: +X
ACCEL: Control
PULSE: 2



UNIT: K-Band Switch
S/N: 002
CALIBRATION
Vertical: 10 gpk/cm
Horizontal: 2 ms/cm
AXIS: +X
ACCEL: Control
PULSE: 3

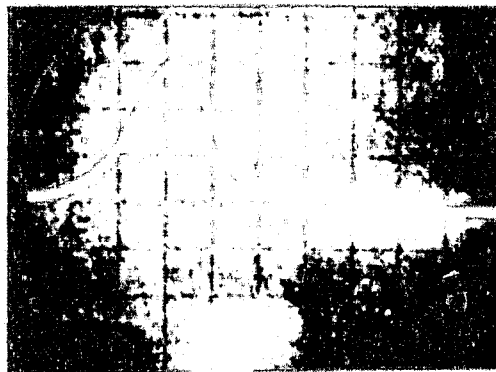


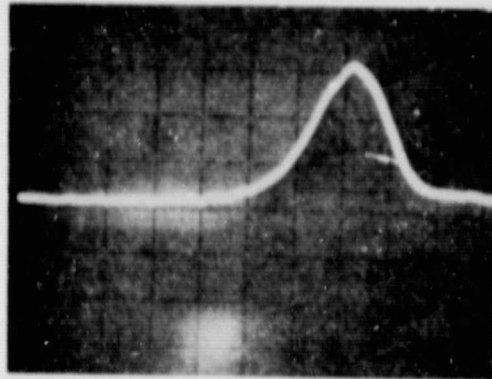
Figure 20a. K-Band Switch Shock Test Data: +X Axis

UNIT: K-Band Switch
S/N: 002
CALIBRATION
Vertical: 10 gpk/cm
Horizontal: 2 ms/cm

AXIS: -X

ACCEL: Control

PULSE: 1

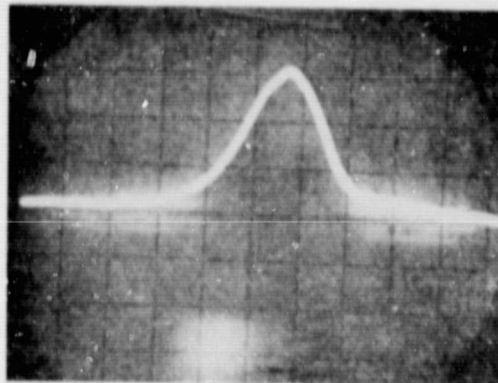


UNIT: K-Band Switch
S/N: 002
CALIBRATION
Vertical: 10 gpk/cm
Horizontal: 2 ms/cm

AXIS: -X

ACCEL: Control

PULSE: 2

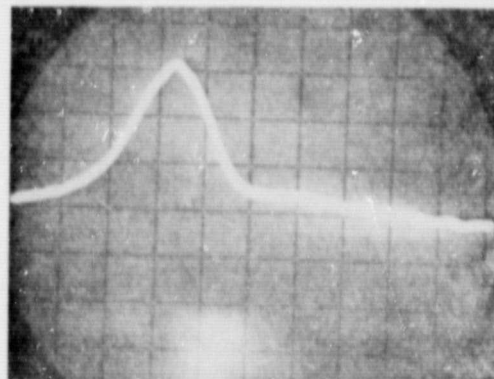


UNIT: K-Band Switch
S/N: 002
CALIBRATION
Vertical: 10 gpk/cm
Horizontal: 2 ms/cm

AXIS: -X

ACCEL: Control

PULSE: 3



ORIGINAL PAGE IS
OF POOR QUALITY

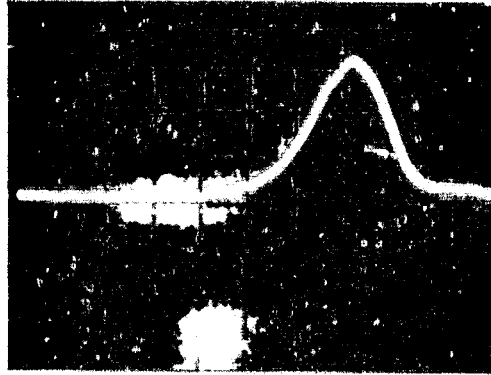
Figure 20b. K-Band Switch Shock Test Data: -X Axis

UNIT: K-Band Switch
S/N: 002
CALIBRATION
Vertical: 10 gpk/cm
Horizontal: 2 ms/cm

AXIS: -X

ACCEL: Control

PULSE: 1

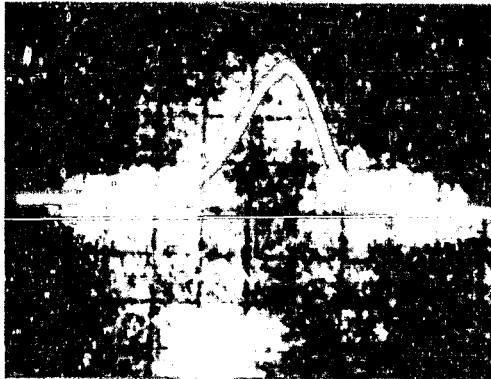


UNIT: K-Band Switch
S/N: 002
CALIBRATION
Vertical: 10 gpk/cm
Horizontal: 2 ms/cm

AXIS: -X

ACCEL: Control

PULSE: 2



UNIT: K-Band Switch
S/N: 002
CALIBRATION
Vertical: 10 gpk/cm
Horizontal: 2 ms/cm

AXIS: -X

ACCEL: Control

PULSE: 3



ORIGINAL PAGE IS
OF POOR QUALITY

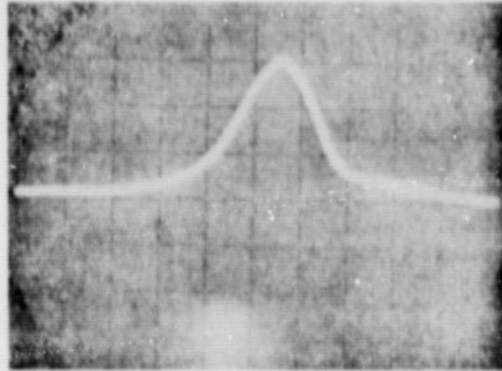
Figure 20b. K-Band Switch Shock Test Data: -X Axis

UNIT: K-Band Switch
S/N: 002
CALIBRATION
Vertical: 10 gpk/cm
Horizontal: 2 ms/cm

AXIS: +Y

ACCEL: Control

PULSE: 1

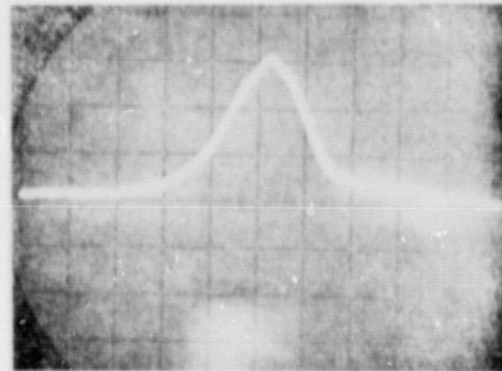


UNIT: K-Band Switch
S/N: 002
CALIBRATION
Vertical: 10 gpk/cm
Horizontal: 2 ms/cm

AXIS: +Y

ACCEL: Control

PULSE: 2



UNIT: K-Band Switch
S/N: 002
CALIBRATION
Vertical: 10 gpk/cm
Horizontal: 2 ms/cm

AXIS: +Y

ACCEL: Control

PULSE: 3

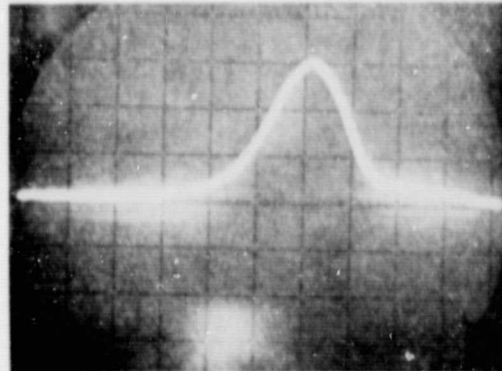


Figure 20c. K-Band Switch Shock Test Data: +Y Axis

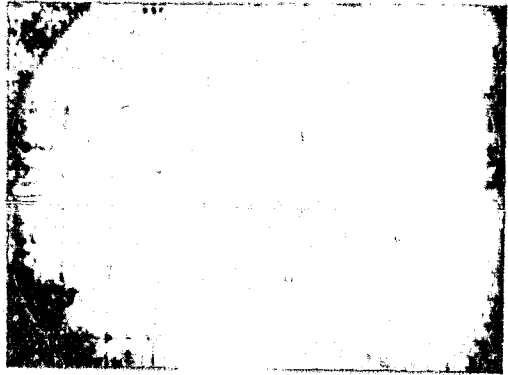
UNIT: K-Band Switch
S/N: 002
CALIBRATION
Vertical: 10 gpk/cm
Horizontal: 2 ms/cm

AXIS: +Y
ACCEL: Control
PULSE: 1



UNIT: K-Band Switch
S/N: 002
CALIBRATION
Vertical: 10 gpk/cm
Horizontal: 2 ms/cm

AXIS: +Y
ACCEL: Control
PULSE: 2



UNIT: K-Band Switch
S/N: 002
CALIBRATION
Vertical: 10 gpk/cm
Horizontal: 2 ms/cm

AXIS: +Y
ACCEL: Control
PULSE: 3

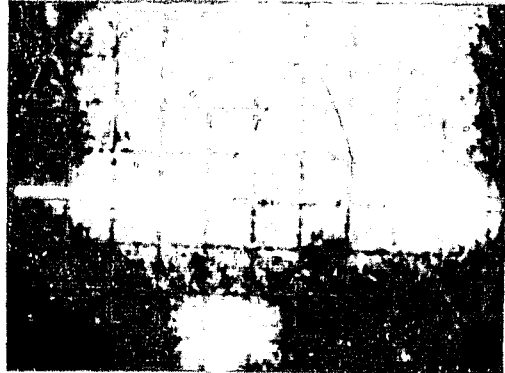


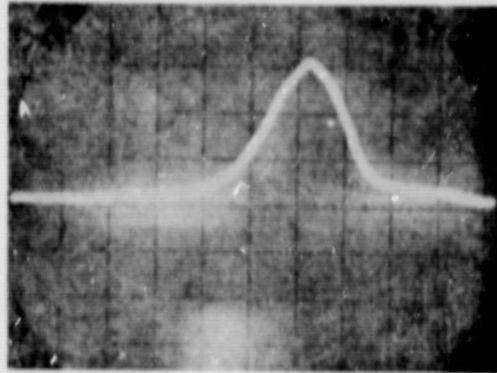
Figure 20c. K-Band Switch Shock Test Data: +Y Axis

UNIT: K-Band Switch
S/N: 002
CALIBRATION:
Vertical: 10 gpk/cm
Horizontal: 2 ms/cm

AXIS: -Y

ACCEL: Control

PULSE: 1

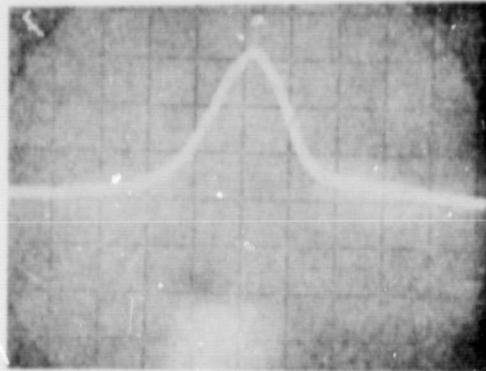


UNIT: K-Band Switch
S/N: 002
CALIBRATION
Vertical: 10 gpk/cm
Horizontal: 2 ms/cm

AXIS: -Y

ACCEL: Control

PULSE: 2

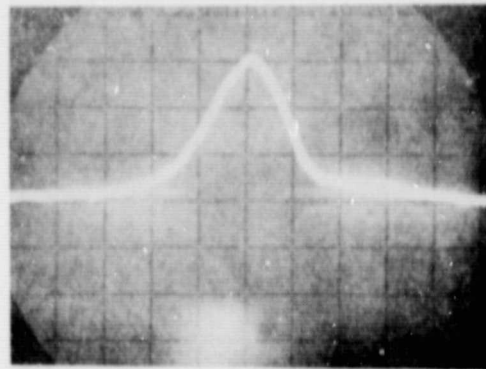


UNIT: K-Band Switch
S/N: 002
CALIBRATION
Vertical: 10 gpk/cm
Horizontal: 2 ms/cm

AXIS: -Y

ACCEL: Control

PULSE: 3



ORIGINAL PAGE IS
OF POOR QUALITY

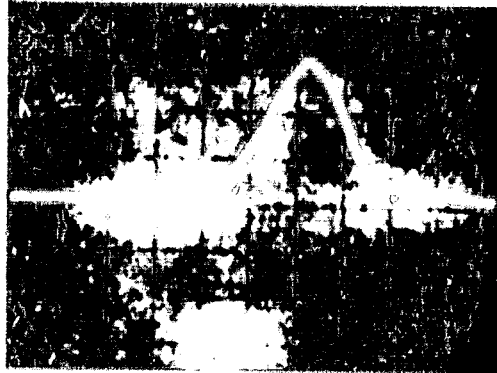
Figure 20d. K-Band Switch Shock Test Data: -Y Axis

UNIT: K-Band Switch
S/N: 002
CALIBRATION
Vertical: 10 gpk/cm
Horizontal: 2 ms/cm

AXIS: -Y

ACCEL: Control

PULSE: 1

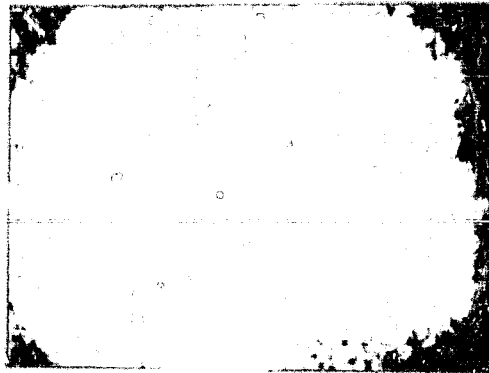


UNIT: K-Band Switch
S/N: 002
CALIBRATION
Vertical: 10 gpk/cm
Horizontal: 2 ms/cm

AXIS: -Y

ACCEL: Control

PULSE: 2

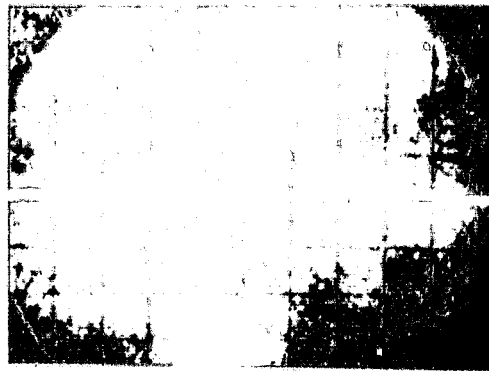


UNIT: K-Band Switch
S/N: 002
CALIBRATION
Vertical: 10 gpk/cm
Horizontal: 2 ms/cm

AXIS: -Y

ACCEL: Control

PULSE: 3



ORIGINAL PAGE IS
OF POOR QUALITY

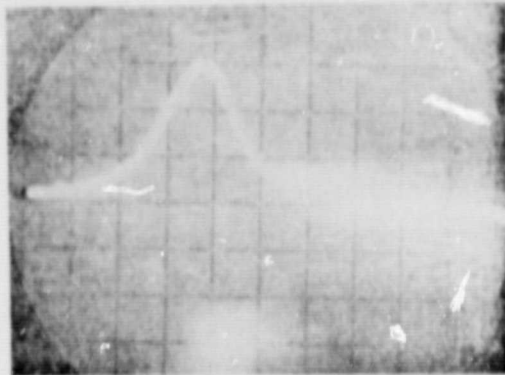
Figure 20d. K-Band Switch Shock Test Data: -Y Axis

UNIT: K-Band Switch
S/N: 002
CALIBRATION
Vertical: 10 gpk/cm
Horizontal: 2 ms/cm

AXIS: +Z

ACCEL: Control

PULSE: 1

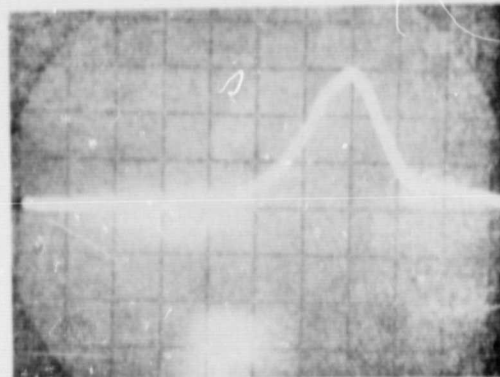


UNIT: K-Band Switch
S/N: 002
CALIBRATION
Vertical: 10 gpk/cm
Horizontal: 2 ms/cm

AXIS: +Z

ACCEL: Control

PULSE: 2



UNIT: K-Band Switch
S/N: 002
CALIBRATION
Vertical: 10 gpk/cm
Horizontal: 2 ms/cm

AXIS: +Z

ACCEL: Control

PULSE: 3

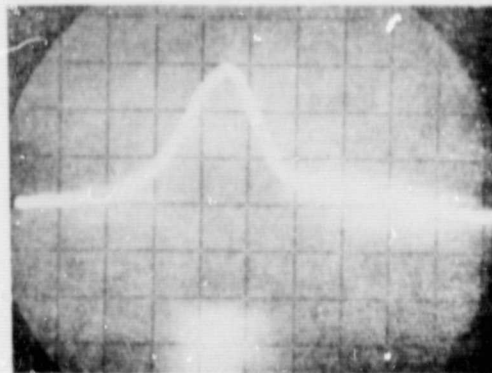


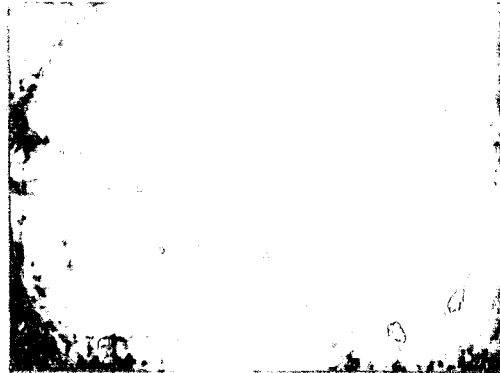
Figure 20e. K-Band Switch Shock Test Data: +Z Axis

UNIT: K-Band Switch
S/N: 002
CALIBRATION
Vertical: 10 gpk/cm
Horizontal: 2 ms/cm

AXIS: +Z

ACCEL: Control

PULSE: 1

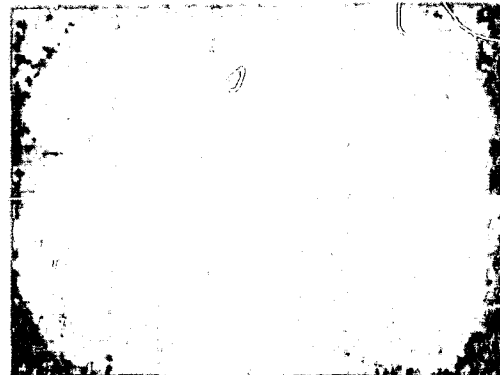


UNIT: K-Band Switch
S/N: 002
CALIBRATION
Vertical: 10 gpk/cm
Horizontal: 2 ms/cm

AXIS: +Z

ACCEL: Control

PULSE: 2



UNIT: K-Band Switch
S/N: 002
CALIBRATION
Vertical: 10 gpk/cm
Horizontal: 2 ms/cm

AXIS: +Z

ACCEL: Control

PULSE: 3

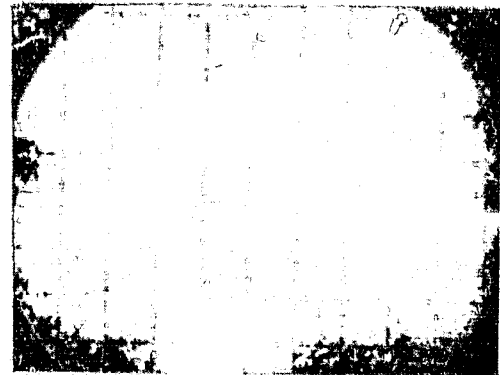


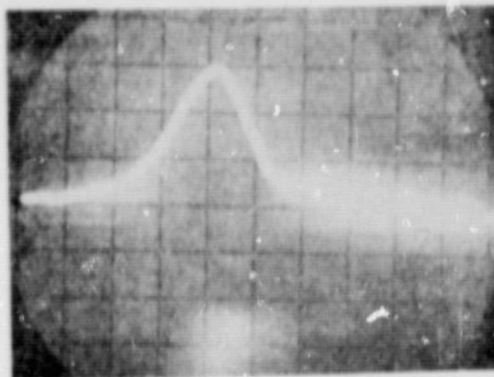
Figure 20e. K-Band Switch Shock Test Data: +Z Axis

UNIT: K-Band Switch
S/N: 002
CALIBRATION
Vertical: 10 gpk/cm
Horizontal: 2 ms/cm

AXIS: -Z

ACCEL: Control

PULSE: 1

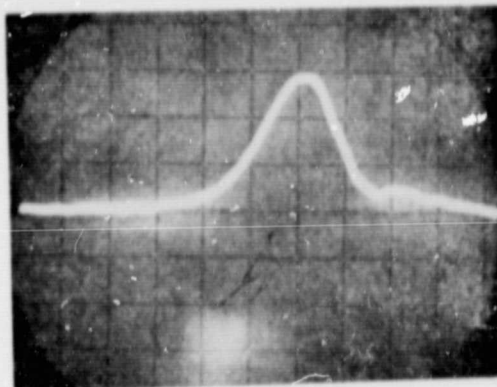


UNIT: K-Band Switch
S/N: 002
CALIBRATION
Vertical: 10 gpk/cm
Horizontal: 2 ms/cm

AXIS: -Z

ACCEL: Control

PULSE: 2

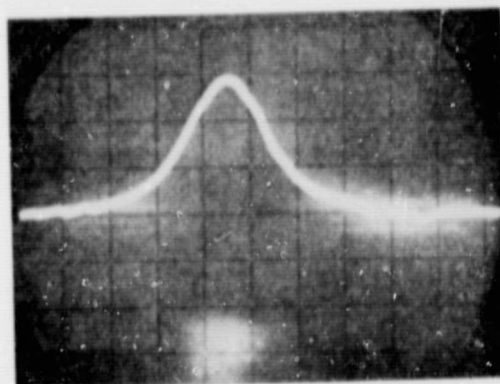


UNIT: K-Band Switch
S/N: 002
CALIBRATION
Vertical: 10 gpk/cm
Horizontal: 2 ms/cm

AXIS: -Z

ACCEL: Control

PULSE: 3



ORIGINAL PAGE IS
OF POOR QUALITY

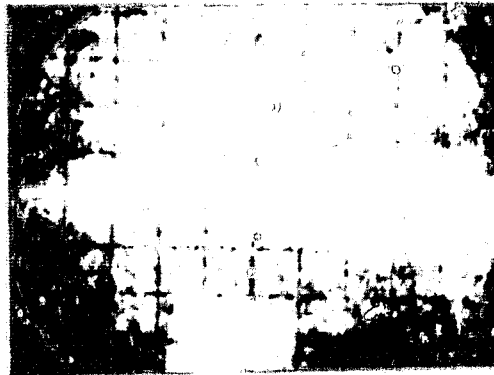
Figure 20f. K-Band Switch Shock Test Data: -Z Axis

UNIT: K-Band Switch
S/N: 002
CALIBRATION
Vertical: 10 gpk/cm
Horizontal: 2 ms/cm

AXIS: -Z

ACCEL: Control

PULSE: 1

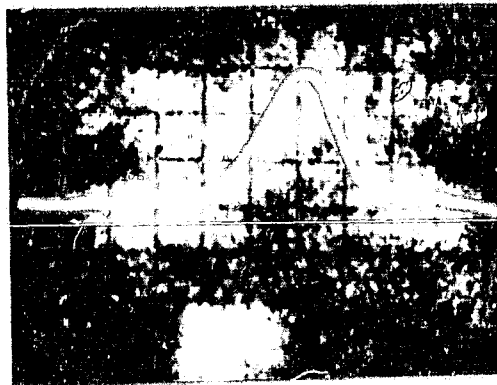


UNIT: K-Band Switch
S/N: 002
CALIBRATION
Vertical: 10 gpk/cm
Horizontal: 2 ms/cm

AXIS: -Z

ACCEL: Control

PULSE: 2



UNIT: K-Band Switch
S/N: 002
CALIBRATION
Vertical: 10 gpk/cm
Horizontal: 2 ms/cm

AXIS: -Z

ACCEL: Control

PULSE: 3



ORIGINAL PAGE IS
OF POOR QUALITY

Figure 20f. K-Band Switch Shock Test Data: -Z Axis

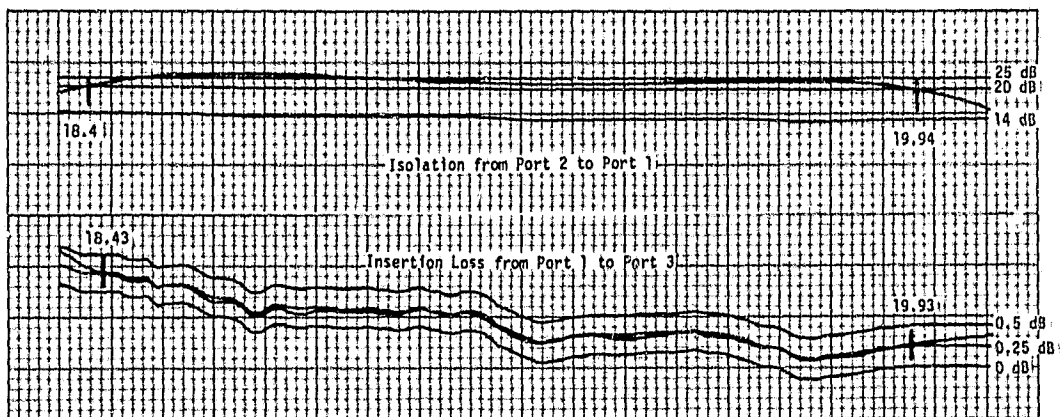
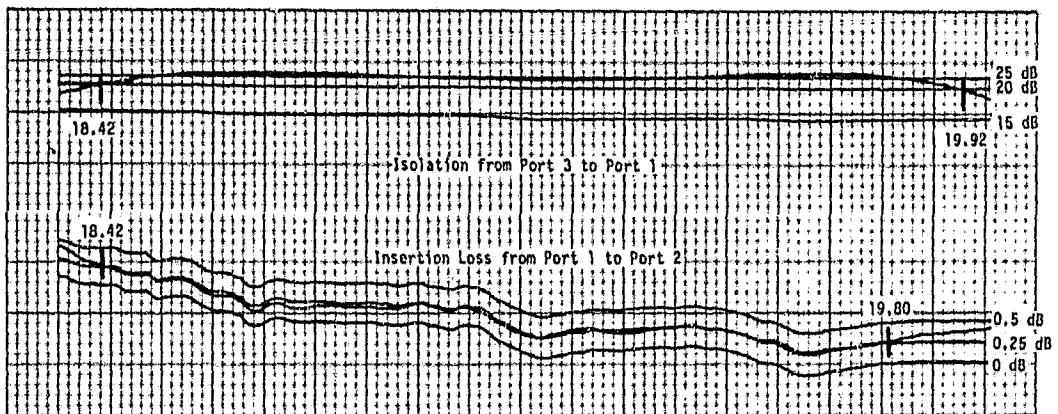
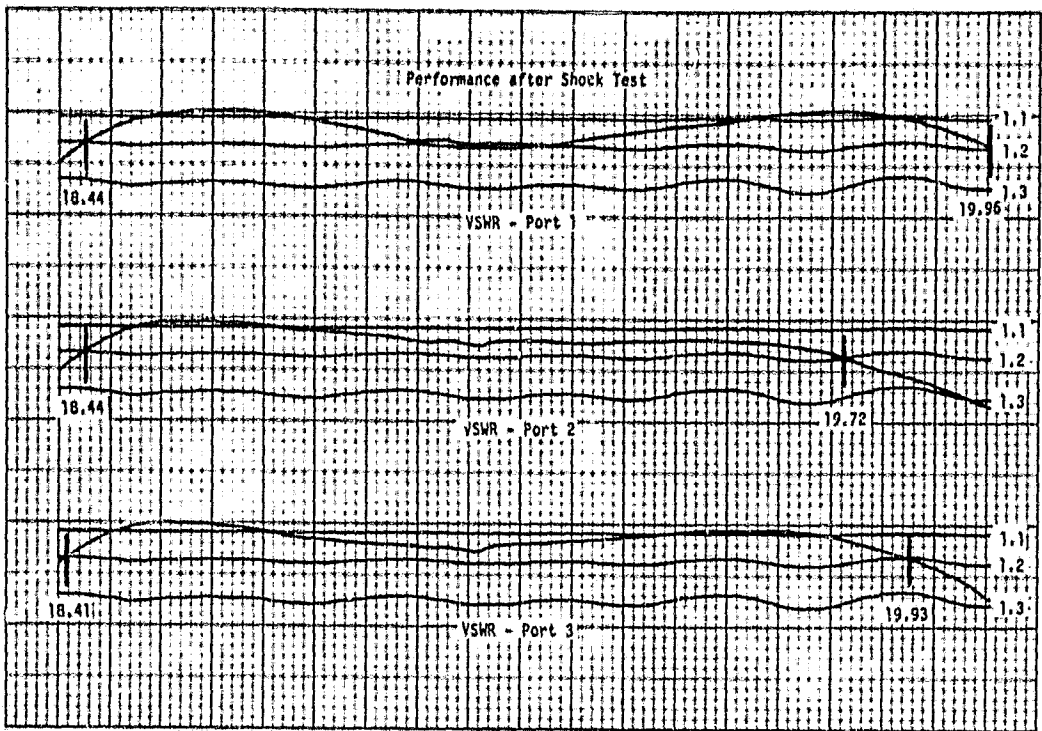


Figure 21. Switch Performance after Shock and Vibration Tests (-2)

3.7 Thermal Test

Prior to delivery of the -1 K-band switch, extensive thermal tests were conducted on the operating unit. The switch was required to operate over a 46C° temperature range from 10°C to 56°C. Furthermore, the unit should demonstrate survivability down to -44°C without performance degradation when returned to operating temperature. The survivability test does not require the switch to be operating.

Shortly after performance measurements on the first switch were completed, thermal testing began. Our testing program involved measuring the room temperature performance as a reference level. The performance was then measured at +56°C and 10°C. A fourth measurement was taken again at room temperature to monitor return to the original performance.

A complete set of thermal measurements was recorded to account for use of any of the ports as an input port. Such testing required a complete temperature cycling for each of the three ports measured. The data obtained is presented in Figure 22.

Survival testing of the K-band switch was conducted by covering the temperature range to -44°C. However, the switch was kept in the circuit since we were positive our circuit would operate due to past experience. Figure 23 shows the insertion loss of the operating switch at -30°C and -44°C. Insertion loss was selected since it is the most sensitive performance parameter.

Upon completion of the survival test, the switch performance was remeasured at room temperature as a comparison to the original performance. The switch displayed identical performance after thermal tests were completed as presented in Figure 24.

The K-band switch passed all of the thermal tests, including survivability. The design of this unit allows switch operation even at the survival temperature. Since the design of this switch is similar to the Landsat and DSCS II switches, which exhibited negligible temperature deviations between component parts, the component temperatures of this junction were not measured.

ORIGINAL PAGE IS
OF POOR QUALITY

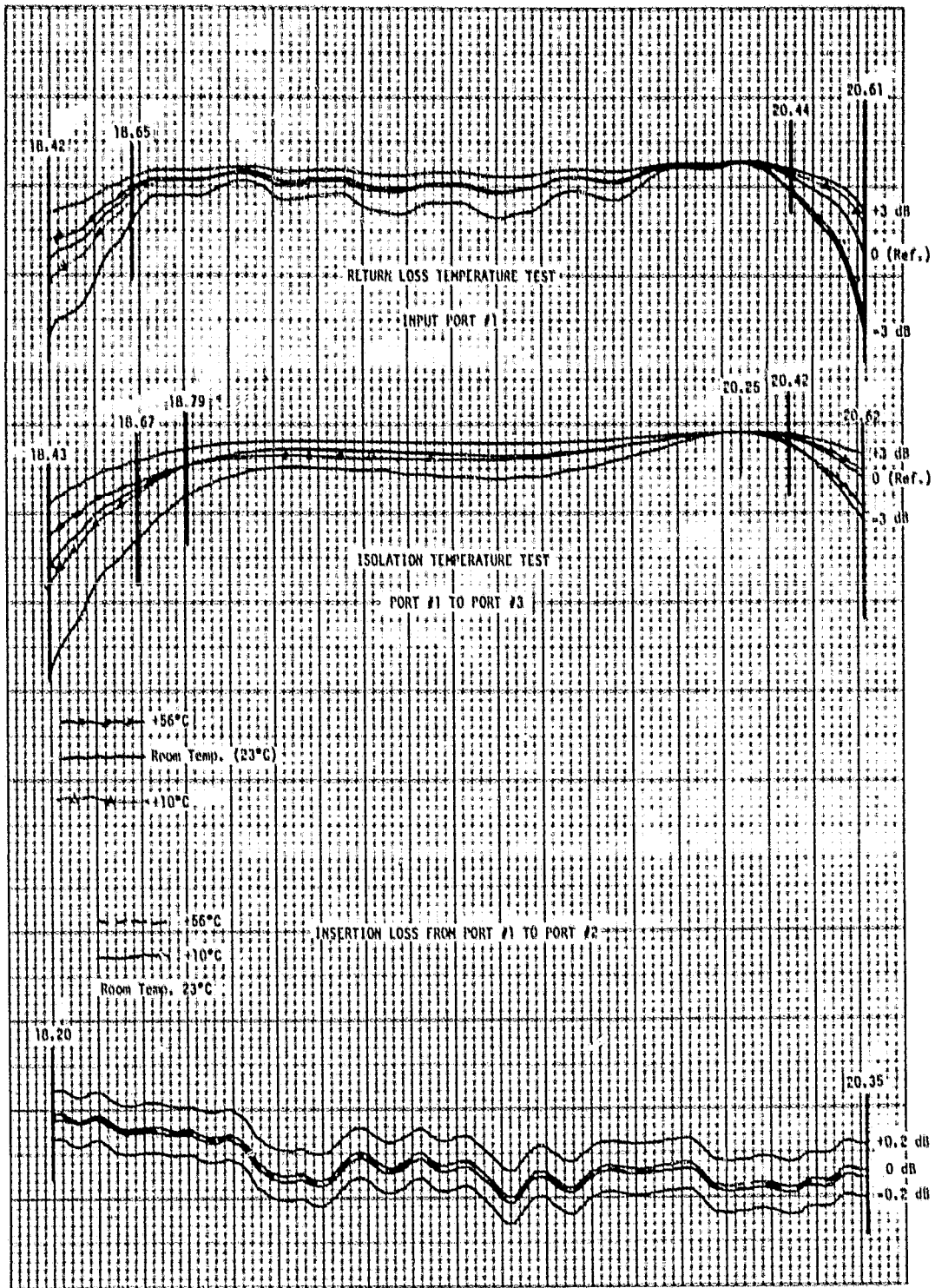


Figure 22a. Performance of K-Band Switch Under Thermal Test (-1) with Port 1 as Input

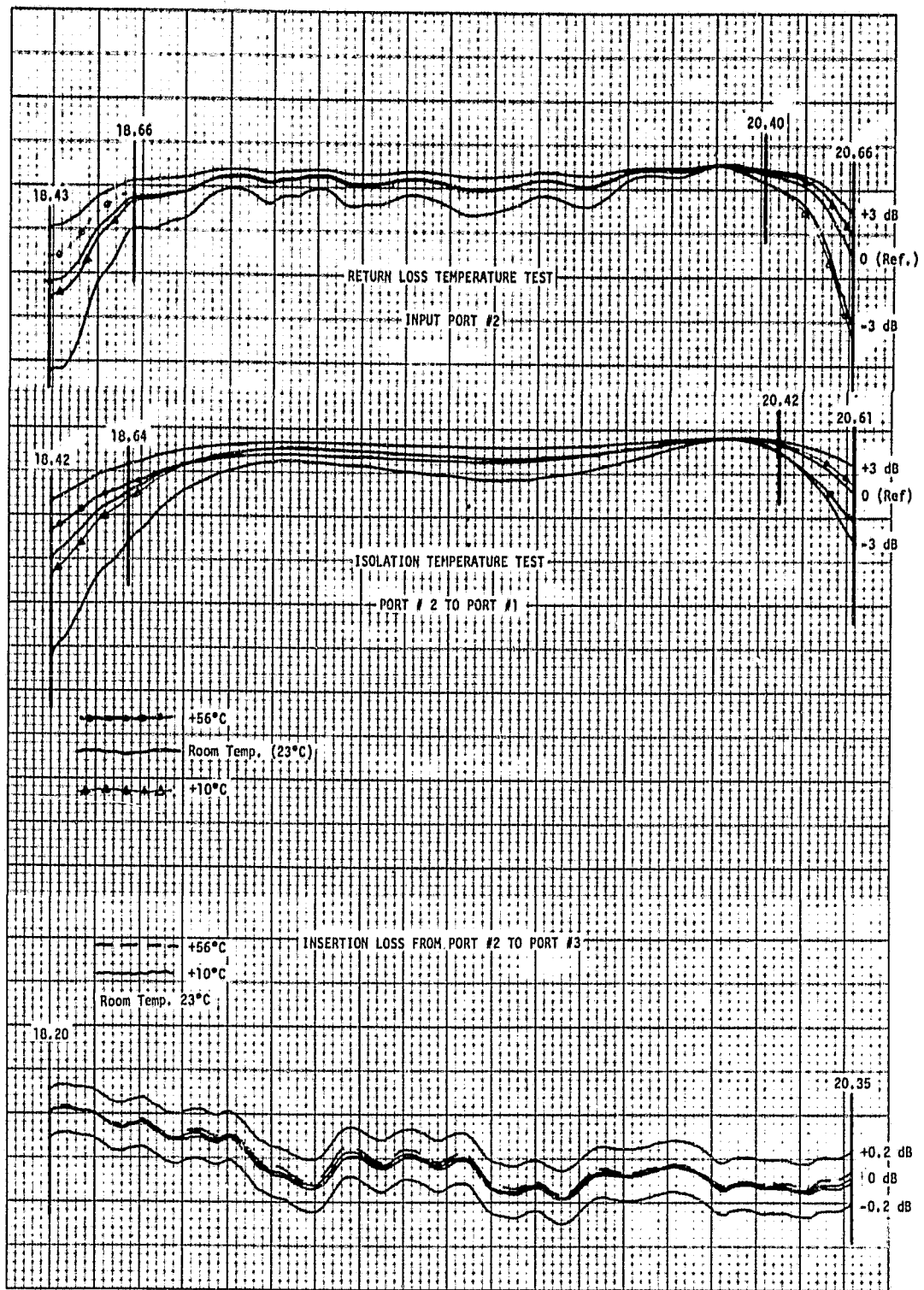


Figure 22b. Performance of K-Band Switch Under Thermal Test (-1) with Port 2 as Input

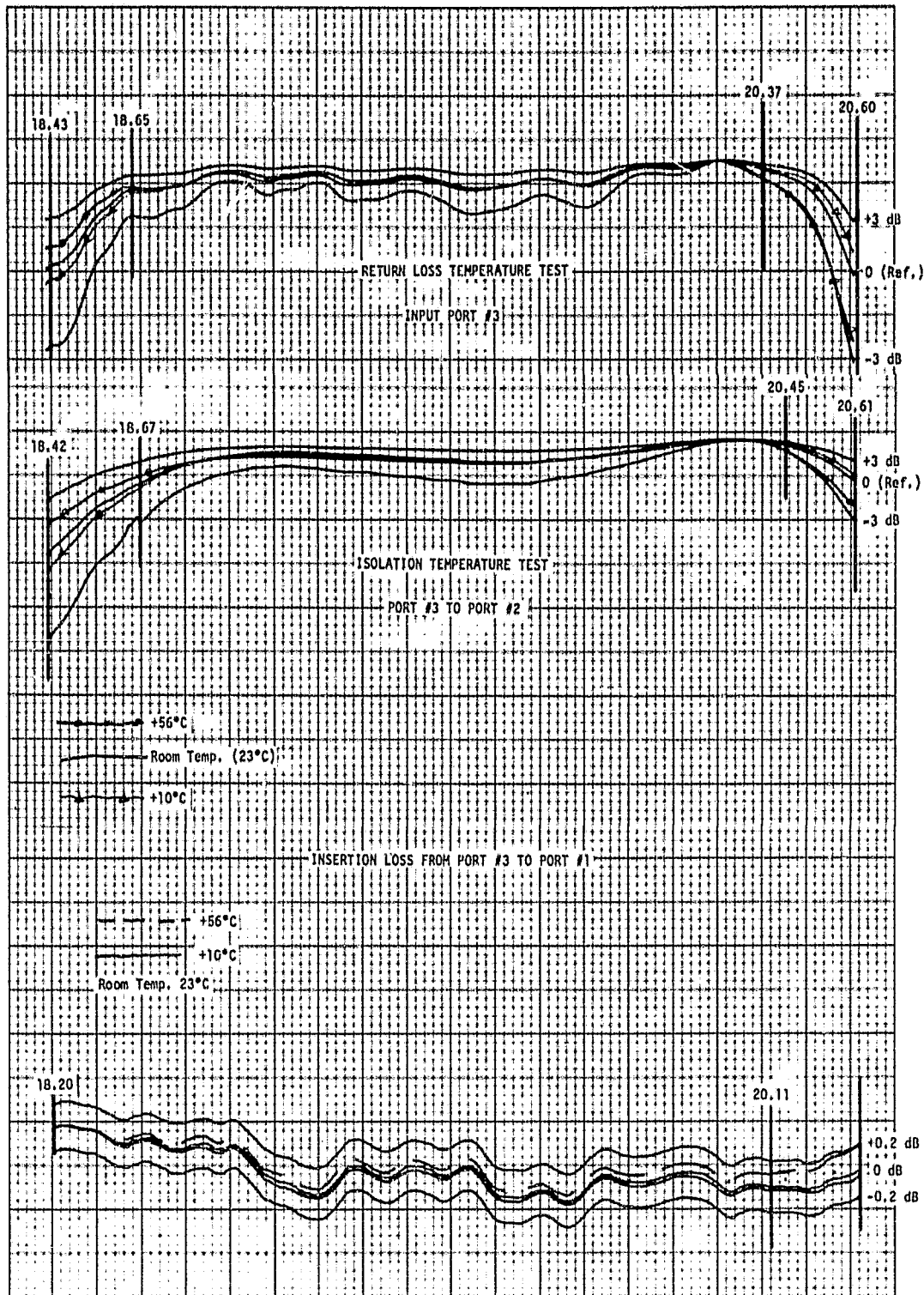


Figure 22c. Performance of K-Band Switch Under Thermal Test (-1) with Port 3 as Input

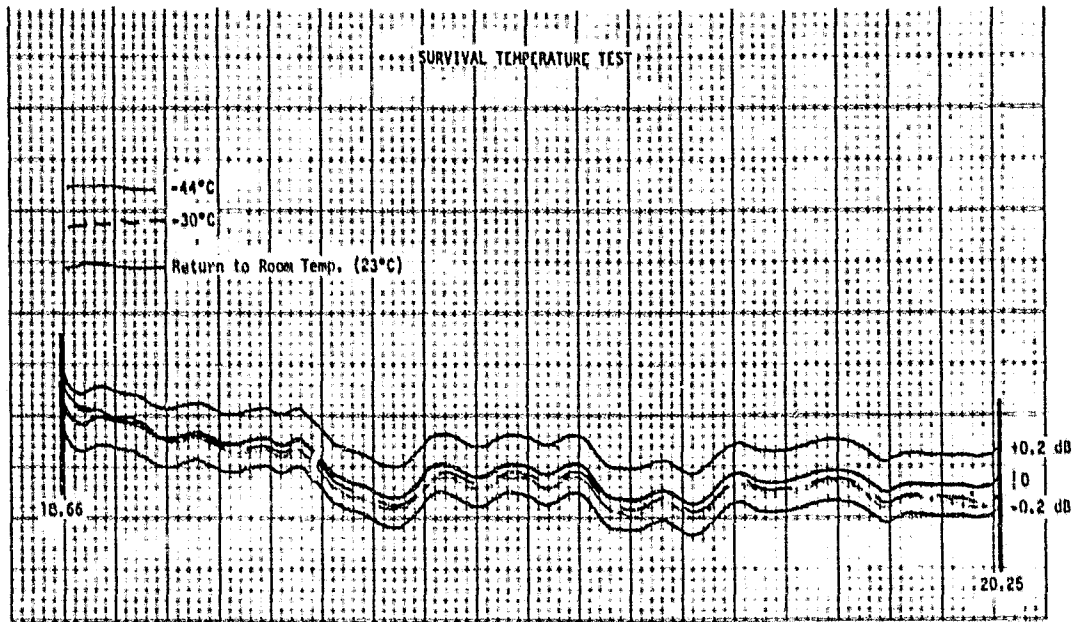


Figure 23. Insertion Loss of K-Band Switch at Survival Temperature (-1)

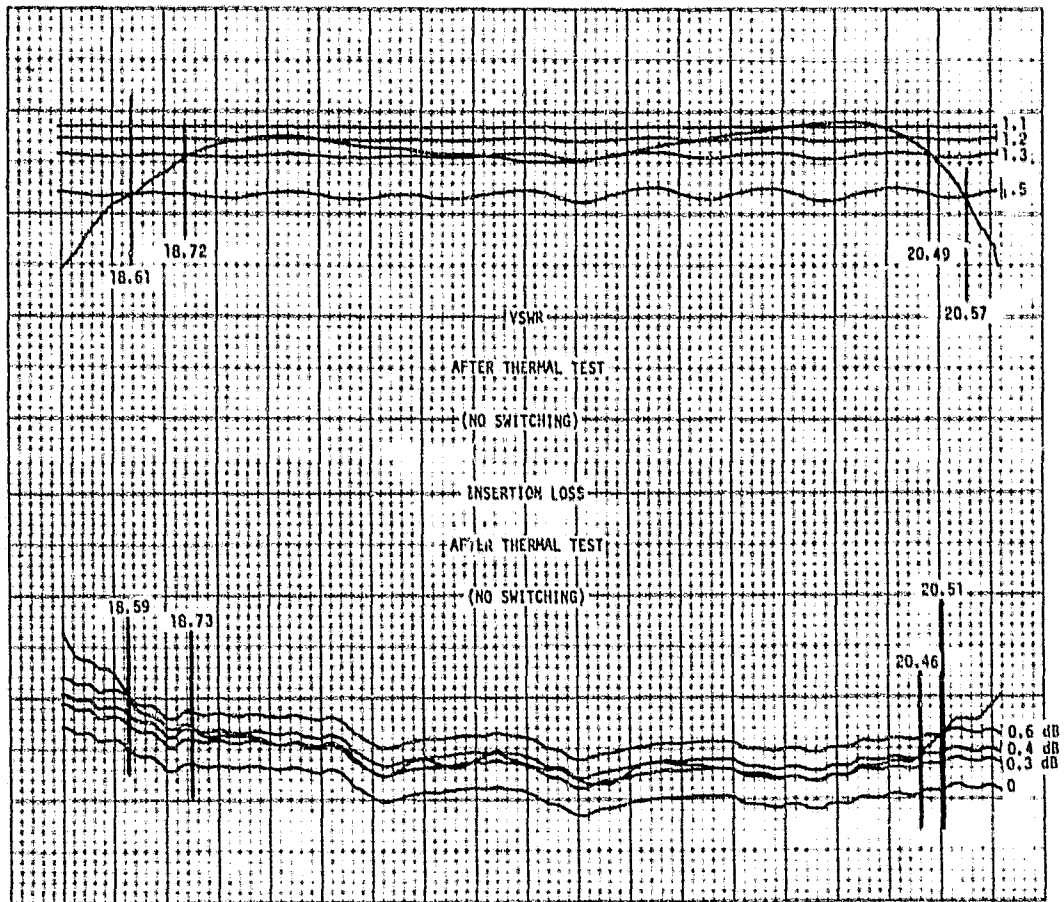


Figure 24. Switch Performance after Thermal Test

ORIGINAL PAGE IS
OF POOR QUALITY

4. CONCLUSIONS

The K-band switch developed for NASA-Lewis was a project requiring delivery of two switches. These light-weight units, whose performance is listed in Table 1, demonstrate extraordinarily low insertion loss and high isolation over a bandwidth of 1.4 GHz. Housed in a single compact unit, as shown in Figure 1, the switching junction and its actuating circuitry met all shock and vibration requirements with no physical damage or performance degradation. In addition, our K-band switch exceeded thermal requirements by operating over a 100C° temperature range (-44°C to +56°C). The units not only operate under adverse conditions, they have a high power handling capability allowing up to 100 W of CW input power.

Extending the operating frequency range of a waveguide latching switch from X-band to K-band involved a year of activity. As the project became more intense, our understanding of the design criteria for switches at higher millimeter wave frequencies grew. There were elements of the design which followed closely the Landsat switch design; other parts of the design were completely contradictory and afforded a new understanding of the influence this higher frequency had on our preliminary design. This knowledge was extremely useful in producing a state-of-the-art device and, furthermore, it allows us an insight into the design of other switches at higher frequencies. In short, the development of this truly unique latching switch was a complete success.